

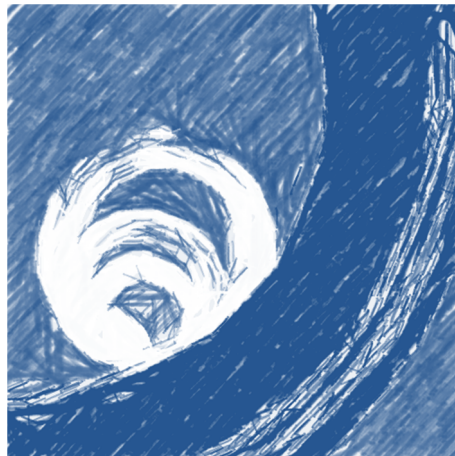


Universidade de  
Aveiro  
Ano 2011

Departamento de Biologia

Ana Raquel Peres  
Marçal

The Gastropod Statolith  
O Estatólito dos Gastrópodes







**Ana Raquel Peres  
Marçal**

**The Gastropod Statolith  
O Estatólito dos Gastrópodes**

Dissertação apresentada à Universidade de Aveiro para cumprimento dos requisitos necessários à obtenção do grau de Mestre em Biologia aplicada, realizada sob a orientação científica do Doutor Carlos Miguel Miguez Barroso, Professor auxiliar do Departamento de Biologia da Universidade de Aveiro, e co-orientação da Sra. Engenheira Fernanda Matos Gonçalves Guimarães, especialista do Laboratório Nacional de Energia e Geologia do Porto.



To my family



## **o júri**

presidente

**Prof. Doutor João António de Almeida Serôdio**

Professor auxiliar do Departamento de Biologia da Universidade de Aveiro

**Doutora Ana Catarina Almeida Sousa**

Investigador Pós-doutoramento, CESAM - Centro de Estudos do Ambiente e do Mar, Universidade de Aveiro

**Prof. Doutor Carlos Miguel Miguez Barroso**

Professor auxiliar do Departamento de Biologia da Universidade de Aveiro

**Engenheira Fernanda Matos Gonçalves Guimarães**

Especialista, Laboratório Nacional de Energia e Geologia



## **agradecimentos**

Este trabalho não representa apenas o meu esforço, mas um conjunto de contribuições, críticas e apoio de verdadeiros amigos, sem os quais a realização do mesmo não seria possível.

Queria começar por agradecer ao professor Doutor Carlos Miguez por ter aceite o desafio de me orientar e ter-me confiado este trabalho. Quero agradecer principalmente por ter acreditado em mim e por me fazer acreditar que eu tinha potencial e capacidade para o fazer. Um grande obrigado por tudo o que me ensinou, pela exigência, pelo apoio total e pela amizade.

Um dia o professor Miguez disse-me que eu iria ter o privilégio de trabalhar com uma aluna sua, extremamente dedicada e uma querida, a Susana. Como sempre o professor não se enganou, porque foi mesmo um privilégio, diria mesmo uma honra, ter tido a oportunidade de ter conhecido a Doutora Susana Galante-Oliveira. Queria agradecer-te Su pela ajuda constante, pelo apoio total, pela dedicação e por tudo o que me ensinaste durante este trabalho. Obrigado por todos os momentos. A ti Su um grande Obrigada.

Um grande obrigado, também, à Engenheira Fernanda Guimarães por todo o apoio e dedicação.

Sem surpresas queria agradecer também ao meu “arqui-inimigo” Mestre Fábio Matos. A ti smeagol um grande obrigado por todos os momentos extra trabalho e extra lazer.

Quero agradecer ao meu namorado, amor e melhor amigo. Sei que estiveste e estarás sempre presente para festejar comigo nos meus bons momentos e para me pôr para cima nos meus momentos menos bons. Obrigado Carlos pelo teu amor, carinho. Obrigado por me fazeres rir. Obrigado por tudo.

## **Agradecimentos (cont.)**

Um grande obrigado a todo o pessoal do LEME: Belucha, São, Lu, Inês, Mariana, Clarinha, Pituxa. Obrigado pela companhia, risadas e as tardes com direito a "jukebox".

Um obrigado especial à Ana Hilário pela ajuda e apoio no laboratório.

Ao Filipe Ribas, obrigado por todo o apoio e colaboração neste trabalho.

Obrigado ao Tiago do Vale pela imagem da capa.

Um obrigado à Carla, Raquel e Carina que não tendo contribuído directamente para este trabalho contribuíram para a minha vida com a sua amizade.

Aos pastores Norton e Raquel, Maria, Dalila, John, Cátia, Carla e Yuri um obrigado a vocês pelo vosso apoio e oração.

Quase a terminar quero agradecer à minha família: pais, manas, cunhados, sobrinhas, tios e primas, um muito obrigado porque sem vocês isto não seria possível. Papá, mamã e Té obrigado por todo o apoio financeiro.

Olho para trás e quero dizer a tantos outros um muito obrigado. Desde colegas, amigos e familiares. Muitos foram aqueles que de certa forma contribuíram para eu chegar até aqui.

E por fim agradeço a Deus. Porque sem Ele eu não estaria aqui.

## **acknowledgements**

This work is not just an individual effort, but a series of contributions, criticisms and support of true friends, without whom this would not be possible.

I would firstly like to thank Professor Carlos Miguez for accepting the challenge of guiding me and trusting in me on this work. Especially I want to thank for believing in me and make me believe that I had potential and capacity to do so. A big "Thank you" for everything you taught me, by the demandingness, the full support and friendship.

One day, Professor Miguez told me I would have the privilege of working with his student, extremely dedicated and sweet, Susan. As always, the teacher wasn't wrong, because it was really a privilege, an honor, to have the opportunity to know Dr. Susana Galante-Oliveira. Su, I want to thank you for the constant help, the total support, all your dedication and for all you taught me during this work. Thank you for all the moments. To you, Su, a big "Thank you".

I would like to thank Engineer Fernanda Guimarães for the support and hospitality at Lneg.

With no surprises, I also want to thank my "archenemy" Master Fabio Matos. To you, Smeagol, a big "Thank you" for all the extra work and extra leisure.

I wish to thank my boyfriend, love and best friend. I know you have been and will always be present to celebrate with me in my good times and to put me up in my not so good moments. Thank you Carlos for your love and affection. Thank you for making me laugh. Thanks for everything.

**Acknowledgements (cont.)**

A big "Thank you" to all the staff at LEME: Belucha, São, Lu, Inês, Mariana, Clarinha, Pituxa. Thank you for the companionship, laughter and the "jukebox" afternoons.

A special "Thank you" to Ana Hilário for the help and support at the lab.

Thanks to Felipe Ribas, for all the support and collaboration on this work.

Thanks to Tiago do Vale by the cover image.

Thanks to Carla, Raquel and Carina, that despite not contributing to this work in particular, contributed to my life with their friendship.

To pastors Norton and Raquel, Maria, Dalila, John, Cátia, Carla and Yuri, thanks for your support and prayers.

Almost finishing, I want to thank my family: parents, sisters, in-laws, nieces, uncles and cousins, thank you because without you this would not be possible. Dad, Mom and Té, thanks for all the financial support.

I look back and I want to thank to many others. Colleagues, friends and family. Many were those who contributed in some way for me to get here.

And finally, thank God. Because without Him I would not be here.

**“The scientist is not a person who gives the right answers,  
he's one who asks the right questions”.**

Claude Lévi-Strauss, *Le Cru et le cuit*, 1964



## palavras-chave

Estatólito, Estatocónia, Estatócisto, Gastrópodes.

## Resumo

O estatólito, análogo aos otólitos, tem-se revelado como um instrumento importante para a determinação da idade e para estudos de crescimento em invertebrados. Localiza-se dentro dos órgãos de equilíbrio, os estatocistos. Apesar de terem sido já bem estudados na classe Cephalopoda, pouco se sabe atualmente sobre a sua estrutura, composição química e possível uso para esclerocronologia na classe Gastropoda. O presente trabalho propõe caracterizar o estatólito em diferentes espécies de gastrópodes, desde os que habitam o ambiente marinho, água doce e terrestre. Procurou-se descrever a localização do estatocisto nas diferentes subclasses e a diversidade de estatólitos existente nesta classe. Verificou-se que nas subclasses Patellogastropoda, Vetigastropoda e Heterobranchia, as espécies apresentam múltiplas estatocónias no interior do estatocisto, que nestes casos se localiza entre os gânglios pedais e pleurais. Na subclasse Caenogastropoda as espécies analisadas apresentam o estatocisto localizado em posição dorsal, sob os gânglios pedais, e apresentam um estatólito por estatocisto. O facto das espécies da subclasse Caenogastropoda terem um estatólito em vez de estatocónia, faz com que estas espécies tenham um maior interesse para estudos de esclerocronologia.

O estatólito dos gastrópodes é uma estrutura aproximadamente esférica de carbonato de cálcio. No seu interior apresenta anéis concêntricos descritos como sendo possíveis anéis de crescimento. Verificou-se que na espécie *Nucella lapillus* o estatólito aumenta proporcionalmente de tamanho com o crescimento do animal, desde o embrião até a fase adulta.

É descrita pela primeira vez a composição química do estatólito de *Nassarius reticulatus* por microanálise com microsonda eletrónica ao longo do raio do estatólito. Os principais elementos químicos presentes são: cálcio (Ca), oxigénio (O), estrôncio (Sr), sódio (Na) e enxofre (S).

**Resumo (cont.)**

Como o estatólito acompanha o crescimento do indivíduo pode guardar inscrito em si um importante registo químico característico do meio em que o animal está inserido, desde o seu nascimento e até ao momento de análise. No entanto, no presente estudo não foram detetadas diferenças significativas nas concentrações dos elementos químicos acima referidos ao longo do raio do estatólito, nos diferentes incrementos analisados, nem foi observado qualquer padrão elementar indicativo de sazonalidade na deposição dos elementos ao longo do raio do estatólito.

**keywords**

Statolith, Statoconia, Statocyst, Gastropods

**Abstract**

The statolith, analogous to the otolith, has been shown to be an important tool for age estimation and growth studies. The statolith is located inside a special chamber named statocyst. The statocyst is the organ of balance of most invertebrates, and is present in a wide range of taxonomic groups of invertebrates. Although there is plenty of research regarding the statoliths/statocysts in the class Cephalopoda, there is a surprising lack of information regarding this structure in the Gastropoda. This work intends to characterize the statolith in gastropods, and assess the diversity of statoliths in this class. It was found that in subclasses Patellogastropoda, Vetigastropoda and Heterobranchia, species present multiple statoconia inside the statocyst, which is located between the pedal and pleural ganglia; in turn, in subclass Caenogastropoda, the analyzed species present a single statolith in each statocyst and the statocyst is located dorsally under the pedal ganglia. The fact that species of subclass Caenogastropoda have one statolith instead of statoconia makes them more useful for sclerochronology studies.

The gastropod statolith is a spherical structure of calcium carbonate that presents concentric rings. Although these concentric rings are reported to have growth rings, the statolith ontogeny is not completely known. It was verified that in *Nucella lapillus* the statolith increases in diameter following the growth of the animal from the embryo to maturity.

For the first time, it was described the chemical composition of the statolith of *Nassarius reticulatus* adults by electron probe microanalysis. The major elements found in statoliths were calcium (Ca), oxygen (O), strontium (Sr), sodium (Na) and sulfur (S).

**Abstract (cont.)**

The statolith increments deposition follow the growth of the animal throughout life and may probably provide an important register of the chemical characteristics of the environment in which the animal live, throughout ontogeny. However, this work could not reveal any significant differences in these elements concentrations throughout the statolith radius (between increments), neither evidences of any particular pattern on the occurrence of elements periodical cycles in the statolith rings.

## Table of Contents

List of Figures .....	2
List of Tables .....	5
Chapter 1 - Introduction .....	7
1.1 References.....	12
Chapter 2 – Gastropod statocyst diversity.....	13
2.1. Introduction.....	13
2.1.1. Gastropod systematics.....	13
2.1.2. Location, structure and function of gastropod statocyst .....	17
2.2. Objectives.....	25
2.3. Materials and Methods.....	25
2.4. Results and Discussion .....	27
2.4.1. Statoconia vs statoliths: the diversity within class gastropoda .....	27
2.4.2. Statocysts location and structure .....	39
2.4.3. Statolith morphology and ontology.....	42
2.5 References.....	46
Chapter 3 - The gastropod statolith chemical composition .....	51
3.1. Introduction.....	51
3.2. The gastropod statolith mineral matrix.....	51
3.3. Objectives.....	53
3.3 Material and methods.....	54
3.4 Results and discussion.....	56
3.5. The gastropod statolith organic matrix.....	65
3.6 References.....	67
Chapter 4 – Conclusion .....	69
4.1 References.....	72

## List of Figures

Figure 1. Gastropod classification after Thiele (1929-1931). The gastropod class was divided into three subclasses: Prosobranchia, Opisthobranchia and Pulmonata. The subclass Prosobranchia was divided into three orders: Archaeogastropoda, Mesogastropoda and Neogastropoda. ....	14
Figure 2. Gastropoda classification after Ponder and Lindberg 1995. The class Gastropoda was first divided into two main divisions Eogastropoda (= Patellogastropoda), and Orthogastropoda. Orthogastropoda includes all the other gastropods. ....	15
Figure 3. Gastropoda classification after Bouchet and Rocroi (2005). The class Gastropoda was divided into six monophyletic groups. ....	16
Figure 4. Gastropod central nervous system (schematic dorsal view, not to scale). Cg: cerebral ganglion; E: oesophagus; Ey: eye; Plg: pleural ganglion; Pg: pedal ganglion; S: statocyst. Adapted from Neusser <i>et al.</i> 2009. ....	17
Figure 5. Statolith and Statoconia. A: Statolith of <i>Nassarius reticulatus</i> showing the external appearance and the concentric layers or rings that can be observed when statolith is grinded down to the centre (here represented in just one quarter of the statolith), adapted from Barroso <i>et al.</i> 2005. Scale bar 50µm. B: Interior wall of statocyst with three statoconia and several cilia of <i>Helix lucorum</i> , extracted from Gorgiladze <i>et al.</i> 2010. Scale bar 10 µm. ....	21
Figure 6. Gastropod tree showing the collected species and their arrangement based on the classification of Bouchet and Rocroi (2005). ....	28
Figure 7. <i>Patella sp.</i> From left to right: Shell dorsal view; shell ventral view; Statocyst open and statoconia. ....	29
Figure 8. <i>Calliostoma zizyphinum</i> . From left to right: Shell apical view; shell apertural view; Statocyst wall and statoconia. ....	30
Figure 9. <i>Gibulla cineraria</i> . From left to right: Shell dorsal view; shell apertural view; Statoconia. ....	30
Figure 10. <i>Gibulla umbilicallis</i> . From left to right: Shell dorsal view; shell apertural view; Statocyst with statoconia. ....	30
Figure 11. <i>Osilinus lineatus</i> . From left to right: Shell dorsal view; shell apertural view; statoconia. ....	30
Figure 12. <i>Aporrhais pespelecani</i> . From left to right: Shell dorsal view; shell ventral view; Statolith with a central nucleus and 4 rings. ....	31
Figure 13. <i>Charonia lampas</i> . From left to right: Shell dorsal view; shell ventral view; Statolith with 13 rings. ....	31
Figure 14. <i>Crepidula fornicate</i> . From left to right: Shell dorsal view; shell ventral view; Statolith with 3 rings. ....	31
Figure 15. <i>Hydrobia ulvae</i> . From left to right: Shell dorsal view; shell ventral view; Statolith with a central nucleus and , metamorphic ring well defined, annual rings not defined. ....	32

Figure 16. <i>Littorina littorea</i> . From left to right: Shell dorsal view; shell ventral view; Statolith with a central nucleus and several rings. ....	32
Figure 17. <i>Nassarius incrassatus</i> . From left to right: Shell dorsal view; shell ventral view; Statolith with a central nucleus, metamorphic ring well defined and annual rings not defined. ....	32
Figure 18. <i>Nassarius reticulatus</i> . From left to right: Shell dorsal view; shell ventral view; Statolith with a central nucleus, metamorphic ring well defined and 4 rings.....	33
Figure 19. <i>Nucella lapillus</i> . From left to right: Shell dorsal view; shell ventral view; Statolith with a central nucleus and annual rings not defined. ....	33
Figure 20. <i>Ocenebra erinacea</i> . From left to right: Shell dorsal view; shell ventral view; Statolith with a central nucleus and annual rings not defined. ....	33
Figure 21. <i>Ocenebrina aciculata</i> . From left to right: Shell dorsal view; shell ventral view; Statolith without defined rings.....	34
Figure 22. <i>Ranella olearium</i> . From left to right: Shell dorsal view; shell ventral view; Statolith with a central nucleus and well defined rings. ....	34
Figure 23. <i>Trivia monacha</i> . From left to right: Shell dorsal view; shell ventral view; Statolith with a central nucleus and rings not defined. ....	34
Figure 24. <i>Aplysia sp.</i> From left to right: Animal dorsal view; animal ventral view; Statocyst open and statoconia.....	35
Figure 25. <i>Helix sp.</i> From left to right: Shell dorsal view; shell ventral view; statoconia.....	35
Figure 26. <i>Nassarius reticulatus</i> . From left to right: shell dorsal view; shell ventral view; animal without shell (the dotted white line indicates the location of the incision); statocysts close to pleural ganglia. ....	40
Figure 27. <i>Patella sp.</i> From left to right: Shell dorsal view. Shell ventral view. Animal head (the dotted white line indicates the location of the incision); Statocysts between pleural and pedal ganglia, see arrows.....	40
Figure 28. <i>Calliostoma zizyphinum</i> . From left to right: Shell dorsal view. Shell ventral view. Statocysts between pleural and pedal ganglia, see arrows.....	40
Figure 29. <i>Aplysia sp.</i> From left to right: animal dorsal view. Animal ventral view (the dotted white line indicates the location of the incision); Statocysts between pleural and pedal ganglia, see arrows. ....	40
Figure 30. <i>Helix sp.</i> From left to right: Shell dorsal view. Shell ventral view. Animal without shell (the dotted white line indicates the location of the incision); Pleural-pedal ganglia. ....	41
Figure 31. <i>Nassarius reticulatus</i> . Histological preparations: statocyst without statolith (A); Statocyst with a statolith (B). A and B: The cells, in the inner of the statocyst, are probably the receptor cells. C: Statocyst in vivo. Statocyst with a statolith. Stc: Statocyst outer wall; Stac-c: Statocyst cavity; c: statocyst inner wall; St: statolith. Scale 100µm.....	41

Figure 32. *Nucella lapillus* ontogeny. A: Capsule with embryos in the first day. B: Capsule with embryos in the beginning of 2<sup>nd</sup> week. C: Embryo in the veliger stage. D: statolith of an embryo with 24 days. .... 43

Figure 33 *Nucella lapillus*. Stn.A: Marégrafo. Stn.B: Costa Nova. The two first points indicates the statolith size with 59 and 77 day of life. The asterisk indicates the time to hatch (approx. on 65<sup>th</sup> day). The line was adjusted visually and may not represent the real trend between the left (early development inside capsules) and right points (animals collected in the field)..... 44

Figure 34. *Nassarius reticulatus*. COMP image showing general aspect of S.1 (A), S.2 (B), S.3 (C), indicating visible rings (MR, R1, R2, R3 and R4) and increments (1, 2, 3, 4 and 5), from the nucleus (N) to the statolith edge. MR: Metamorphic ring; R1: First ring; R2: Second ring; R3: Third ring; R4: Fourth ring; N: Nucleus; 1: First increment; 2: Second increment; 3: Third increment; 4: Fourth increment; 5: Fifth increment..... 57

Figure 35 EDS Spectrum indicating the most representative elements in *Nassarius reticulatus* statoliths. C: Carbon; Ca: Calcium; Mg: Magnesium; Na: Sodium; O: Oxygen; S: Sulfur; and Sr: Strontium. .... 58

Figure 36 WDS Spectra indicating the most representative elements present in *Nassarius reticulatus* statoliths. C: Carbon; Ca: Calcium; Na: Sodium; O: Oxygen ..... 58

Figure 40 Line profiles of C, Sr, Ca and O along S.3 radius. Overlapping profiles (black vertical lines) are indicated the S.3 dark rings position. On the bottom of the figure there is also part of Figure 35 (S.3 COMP image) indicating the exact position of S.3 dark rings (MR, R1, R2, R3 and R4). .... 63

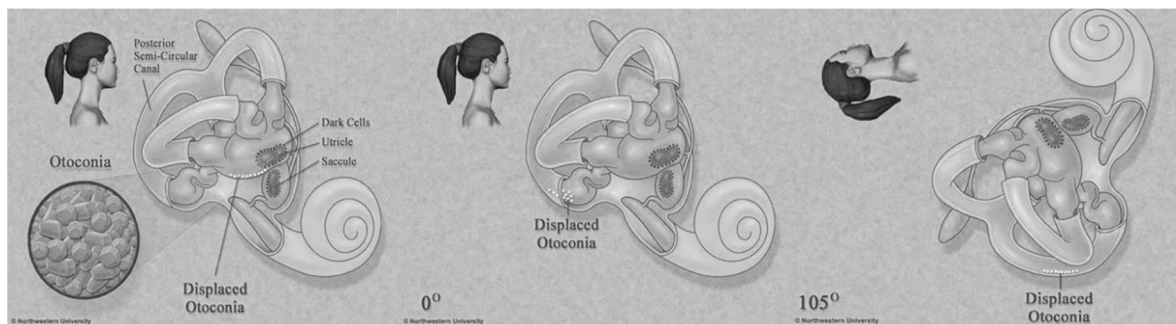
## List of Tables

Table 1. Statocyst location in some gastropods species.....	19
Table 2. Taxonomic tree of the species used in the present work. Statoconia:  Statolith:  .....	36
Table 3. Summary of the records found in literature for minor and trace elements detected in statoconia and statoliths. Elements are presented by species and respective references are also indicated.	52
Table 4 Elemental analysis of <i>Nassarius reticulatus</i> adult statoliths (S.1, S.2 and S.3) by EPMA. Maximum (Max) and minimum (min) concentrations detected for each element (ppm) within the set of analyses performed .....	59
Table 5 Elemental analysis of statolith S.1 by EPMA. Mean concentrations of each element (ppm) by increment (see Figure 1) and respective coefficient of variation (CV). The value shaded in grey (Mg concentration in increment 4) was only detected at one of the three points analysed. ....	60
Table 6 Elemental analysis of statolith S.2 by EPMA. Mean concentrations of each element (ppm) by increment (see Figure 2) and respective coefficient of variation (CV).....	60
Table 7 Elemental analysis of statolith S.3 by EPMA. Mean concentrations of each element (ppm) by increment (see Figure 3) and respective coefficient of variation (CV). The value shaded in grey (Mg concentration in increment 3) was only detected at one of the three points analysed. -: not detected.....	61
Table 8 Statistical comparisons of each element concentration between different increments of statoliths S.1, S.2 and S.3. - : not performed. ....	61
Table 9 Minor and trace elements in statolith S.3 detected by EPMA. Mean concentrations of each element (ppm) by increment (see Figure 3) and respective coefficient of variation (CV). (* the values are not means since the element was only detected at one of the three analyses carried out at each increment. -: not detected. ....	64



## Chapter 1 - Introduction

If we would ask to a common person to list the main types of senses (or sensory modalities) of humans, the most probable answer would be the sight, hearing, touch, smell and taste, which represent the “five senses” concept of Aristotle lost in the antiquity. In fact, people can easily name a body part used for each of these senses as they can see or feel their eyes, ears, skin, nose and tongue, and they can recognize the use of each of them to explore specific properties of objects in the surrounding environment. If we would then ask them to explore a set of objects spread in a given space they would move to get close to the objects and should recognize that they were using another crucial sense that helps them to orientate and to control their equilibrium. In fact, while moving they feel accelerations in many directions (top/bottom, front/back, right/left) and they keep postural control in relation to gravity. This further sense is provided by a specific mechanoreceptor organ located in the human inner ear that provides perception of acceleration and position (see Figure 1).



**Figure 1. Inner ear: Cochlear and Semicircular canals. According to the movement of the body, otoconia move within the semicircular canals. Adapted from Hain 2011.**

The type of georeceptor organ described above is ubiquitous in the living world and has evolved since the dawn of life on earth. In plants (see Figure 2), the plastids, known as amyloplasts, act for sensing gravity (Morita 2010).

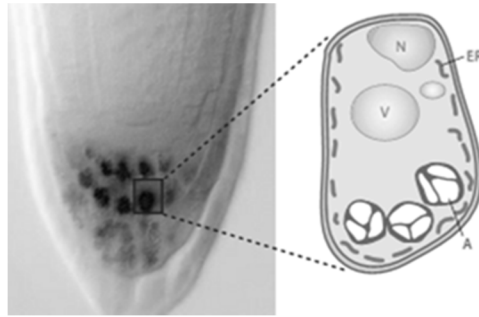


**Figure 2.** Left: Root structure. Amyloplasts are visible in columella cells in the root cap. Right: Structure of the columella cell, showing the nucleus (N), vacuole (V), amyloplast (A), and endoplasmic reticulum (ER). Adapted from Morita 2010.

Even free living cells like the protists are able to perceive gravity either by intracellular receptors (statocyst like organelles, see below), heavy cell organelles (such as the nucleus) and/or by sensing the cell mass by means of ion channels located in the cell membrane (Bräucker *et al.* 2002). An evolved georeceptor organ appears in metazoans. The simplest form of this organ - the statocyst - occurs in the invertebrates and consists of a chamber containing a free solid granule or a mass of cohering grains, generally designated as statolith. The displacement of the statolith due to changes in the position of the animal stimulates local sensory cells, indicating the body position in respect to gravity. This organ has developed considerably through evolutionary progression from invertebrates to vertebrates and despite great differences in its ontogeny and structure, the physical principle of functioning remained basically the same.

The simplest metazoans showing statocysts are the Cnidaria and the Ctenofora. For instance, the scyphozoan jellyfishes possess statocysts within club-shaped structures called rhopalia, which are distributed along the margins of the swimming bell. In each rhopalia a tubular piece of tissue hangs free with a statocyst at its terminal edge. Dense aggregations of nerve tissue are associated with the rhopalia and control the rhythmic contraction of the swimming bell. When the animal tilts in a given direction the statoliths stimulates certain sensory cilia. This generates action potentials in associated nerve cells that will trigger contractions of the bell in order to re-establish the vertical posture (Pechenik 1996). The Ctenofora is another group of animals at about the same level of organization than cnidarians, popularly known as sea-gooseberries or comb-jellies

(Fretter and Graham 1976) that possess one apical statocyst (Hickman *et al.* 2006) that also functions as a gravity sense organ. The same general type of statocysts are present in most of other invertebrates, such as annelids, crustaceans, molluscs, echinoderms, tunicates, etc. (Fretter and Graham 1976; Purchon 1977; Barnes 1980), though the microstructure and shape of the statocyst varies amongst taxa. The statolith may consist of a single or multiple small calcareous concretions (e.g. molluscs) or cohering sand grains (e.g. crustaceans) (Fretter and Graham 1976). They may even consist of diatom shells and quartz grains covered by chitinous material in some polychaete families (Barnes 1980). Statocysts may also present a closed structure (e.g. molluscs) or may retain an opening to the exterior (e.g. crustacean). In the latter case, the grains of sand that lie inside the statocyst of crustaceans, which function as statolith, are lost in each molt and new ones are picked up through the statocyst opening after ecdysis (Hickman *et al.* 2006). Although in most invertebrate taxa statocysts typically present a simple saclike appearance, in cephalopods they are more complex and show an amazingly close resemblance to vertebrate organs (e.g. semicircular canals in *Octopus* spp.) (Anken and Rahmann 2002). The most evolved equilibrium sense organs definitively occur in vertebrates. Inner ears of vertebrates present three looping semicircular canals perpendicular to each other for the detection of angular acceleration (or rotation of the head) plus three chamber containing otoliths or statoconia in lower vertebrates (utricle, saccule and lagena for the perception of linear acceleration/gravity and sound) or two chambers with statoconia and a lagena/cochlea without a otolith or statoconia for sound perception in higher vertebrate animals. In the above chambers there are patches of sensory and supportive cells called macula. The macula is associated to underlying sensory neurons and in the opposite side has a cupula that is made heavy by deposits of calcareous material: in fishes these deposits can form a solid mass (the otolith) while in amphibians, reptiles, birds and mammals the deposits remain as hundreds of thousands minute calcium carbonate crystals (the statoconia or otoconia). When the head of the animal moves, the otoliths or otoconia tend to slide over the macula in response to gravity, producing a force to which hair cells are sensitive and allow the detection of postural position and acceleration (Hildebrand 1974; Anken and Rahmann 2002).

Besides the general interest that the above mentioned equilibrium sense organs may represent for physiology, ethology, taxonomy and other areas of biological science, the present dissertation aims to explore the usefulness of gastropod statoliths for sclerochronology. The sclerochronology is a field of science dedicated to the study of physical and chemical variations in calcified structures of organisms (e.g.: fish otoliths, bones and scales, mollusc shells, corals, etc.) and the temporal context in which they form. It is central for age estimation and growth analysis in studies of biology and fisheries management, to deduce organism life history traits or to reconstruct records of environmental and climatic change through space and time. Barroso *et al.* (2005) demonstrated that statoliths of adult gastropod molluscs can be used in sclerochronology. Based on samples collected from the seacoast of Aveiro (Portugal), these authors showed that the gastropod species *Nassarius reticulatus* possesses two statocysts, each containing a spherical statolith of calcium carbonate of up to 0.22 mm in diameter that can provide information about the age and growth of this species. Richardson *et al.* (2005a, b) showed that the gastropods *Neptunea antiqua* and *Polinices pulchellus* possessed similar statoliths that could be used for age determinations. Later, Chatzinikolaou and Richardson (2007) corroborated the results obtained by Barroso *et al.* (2005) for *N. reticulatus* collected from United Kingdom seacoast.

The application of adult gastropod statoliths in sclerochronology is recent and may present many advantages comparing to the most traditional organisms that have been used in marine sclerochronology such as fish, bivalves cephalopods and corals. One advantage is the fact that gastropods are sedentary or poorly mobile organisms, unlike fish or cephalopods, and so they can describe the physical-chemical composition of the marine environment in a particular location along time. A second advantage is the fact that, unlike the shells of bivalves or gastropods, the statoliths are internal structures that are protected from erosion and mechanical/chemical stress and so they can register accurately information on the marine environment and can also provide good age estimations. Many aspects are still unexplored in the literature, namely if statoliths can be universally used for describing the age and growth in class Gastropoda. This is important because in most gastropod species the outer shell surface has few rings that can be used

reliably for age estimation and their detection in the conical spired shells of gastropods is complicated without serial sectioning. The annual rings present in gastropod statoliths may overcome these difficulties as demonstrated by Barroso *et al.* (2005), Richardson *et al.* (2005a, b) and Chatzinikolaou and Richardson (2007). In this dissertation it is pretended to advance furthermore this topic with the attempt to relate the rings observed in the statolith through visual/image analysis with the chemical analysis of the statolith, assuming that seasonal variation of chemical fingerprints may provide a good validation of the observed annual rings.

The general objective of this thesis is to contribute to the advance of the techniques in sclerochronology and to improve our understanding regarding the diversity and the microstructure of gastropod statolith. The specific objectives are: (i) to provide a comprehensive characterization of the type, shape, microstructure and chemical constitution of the statoliths in class Gastropoda, and to (ii) improve and expand the use of statoliths for age and growth assessments in class Gastropoda. The thesis is organised in four chapters. Chapter 1 (the current one) is the general introduction of the theme of the thesis, where the main objectives of the work are defined. Chapter 2 characterizes the diversity of statoliths that occur in different species of gastropods collected in Aveiro (NW Portugal) and the adjacent seacoast. Chapter 3 describes the chemical composition of statoliths of *Nassarius reticulatus* and addresses its usefulness for age determinations and environmental monitoring. Chapter 4 states the major conclusions of the current work and prospects complementary work to be developed in the future.

## 1.1 References

- Anken, R. H. and Rahmann, H. (2002). Gravitational zoology: how animals use and cope with gravity. In *Astrobiology. The Quest for the Conditions of Life* (ed. G. Horneck and C. Baumstark-Khan), pp. 315 -333. Berlin: Springer.
- Barnes RD (1980). *Invertebrate zoology*, 4th edn. Saunders College Publishing, Philadelphia.
- Barroso, C. M., M. Nunes, *et al.* (2005). The gastropod statolith: a tool for determining the age of *Nassarius reticulatus*. *Marine Biology* 146(6): 1139-1144.
- Bräucker, R., Cogoli, A. and Hemmersbach, R. (2002). Graviperception and graviresponse at the cellular level. In *Astrobiology. The Quest for the Conditions of Life.* (Ed. C. Baumstark-Khan and G. Horneck), pp. 284-97. Berlin: Springer Verlag .
- Chatzinikolaou, E. and Richardson, C. A (2007). Evaluating growth and age of netted whelk *Nassarius reticulatus* (Gastropoda: Nassariidae) using statolith growth rings. *Marine Ecology-Progress Series* 342:163-176.
- Fretter, V. and Graham, A. (1976). *A functional anatomy of invertebrates*. London: Academic Press.
- Hain, T. C. (2011). Benign paroxysmal positional vertigo Accessed through: <http://www.dizziness-and-balance.com/disorders/bppv/movies/Debris-Redistribution.gif>.
- Hickman, C. P. Jr., Roberts, L. S., Larson, A. (2006) *Integrated Principles of Zoology* (13rd edition). McGraw-Hill Publishers: XXIII : 882.
- Hildebrand, Milton (1974). *Analysis of Vertebrate Structure*. New York and London: John Wiley & Sons.
- Morita, M. T. (2010) Directional Gravity Sensing in Gravitropism. *Annual Review of Plant Biology*, Vol 61: 705-720.
- Ponder, W. F. and D. R. Lindberg (2008). *Phylogeny and Evolution of the Mollusca*. California, University of California Press, USA.
- McArthur, A. G., Harasewych, M. G. (2003). *Molecular Systematics and Phylogeography of Mollusks*, 140-160. (<http://hdl.handle.net/10088/16793>)
- Pechenik, J. (1996). *Biology of invertebrates*. Dubuque: Wm. C. Brown Publishers.
- Purchon RD (1977). *The biology of the Mollusca*. International series of monographs in pure and applied biology zoology, vol 57, 2nd edn. Pergamon, Oxford.
- Richardson, C. A., Kingsley-Smith, P. R., Seed, R., Chatzinikolaou, E. (2005b). Age and growth of the naticid gastropod *Polinices pulchellus* (Gastropoda: Naticidae) based on length frequency analysis and statolith growth rings. *Marine Biology* 148(2): 319-326.
- Richardson, C. A., Saurel, C., Barroso, C. M., Thain, J. (2005a). Evaluation of the age of the red whelk *Neptunea antiqua* using statoliths, opercula and element ratios in the shell. *Journal of Experimental Marine Biology and Ecology* 325:55 – 64.

## **Chapter 2 – Gastropod statocyst diversity**

### **2.1. Introduction**

The Mollusca is the second largest phylum of the kingdom Animalia and one of its most diverse groups with about 200,000 living species (Ponder and Lindberg 2008). In terms of number of species, Gastropoda is considered the major class of Mollusca (80% of all molluscs are gastropods) due to the great evolutionary radiation suffered, and is also the second largest class of the animal kingdom. This group is generally characterized by having a single shell, an operculum and a larvae undergoing torsion. Gastropods vary in external shape, size, behavior, anatomy and physiology, and show an almost global distribution, from marine and freshwater to terrestrial environments (Campbell 2008; Ponder and Lindberg 2008).

#### **2.1.1. Gastropod systematics**

To better understand the diversity of statocysts and statolith/statocconia in gastropods, it is first necessary to describe the biodiversity in class gastropoda and clarify the taxonomic nomenclature here adopted. The gastropods biodiversity has been traditionally grouped into three subclasses – Prosobranchia, Opisthobranchia and Pulmonata – following Milne-Edwards's (1848). Thiele (1929-31) (see Figure 3) adopted Milne-Edwards's (1848) classification but further subdivided the Prosobranchia into three orders: Archaeogastropoda, Mesogastropoda, and Stenoglossa (this last one renamed Neogastropoda by Wenz 1938-44) (Franc 1968; McArthur and Harasewych 2003).

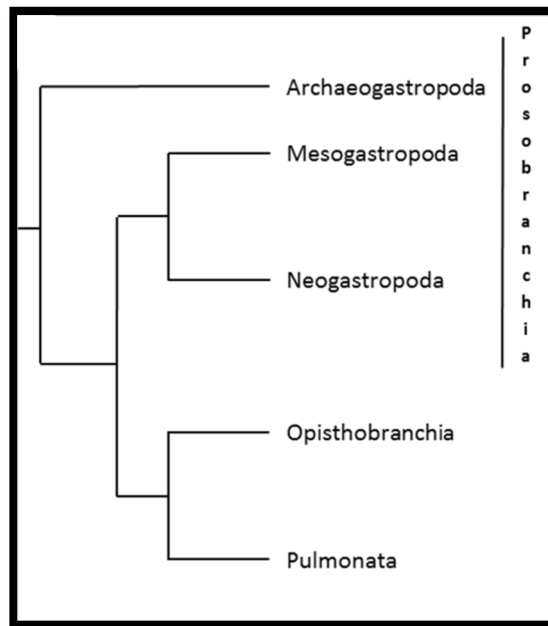


**Figure 3. Gastropod classification after Thiele (1929-1931). The gastropod class was divided into three subclasses: Prosobranchia, Opisthobranchia and Pulmonata. The subclass Prosobranchia was divided into three orders: Archaeogastropoda, Mesogastropoda and Neogastropoda.**

This was until recently the main classification accepted and followed in most textbooks. However, gastropods classification has evolved in the recent years due to: (i) the discover of new taxa, especially in deep-sea environments; (ii) the rapid increase of new data provided by new morphological and molecular techniques; and (iii) the development of new methodologies for data analysis and phylogenetic hypotheses generation (McArthur and Harasewych 2003; Ponder and Lindber 2008).

One important change to the above classification (hereafter designated as "old classification") was proposed by Yonge's (1947) that divided the Aspidobranchia (prosobranchs with bipectinate ctenidia) into four groups: (i) true limpets (now described as Patellogastropoda), (ii) ancient marine snails (now described as Vetigastropoda), (iii) caenogastropods and (iv) neritoideans. Although the position of these groups has changed in the following years, the main contribution of this scheme was the recognition of the neritoideans (equivalent to Neritimorpha).

Other major modification to the old classification was proposed by Cox (1960) and consisted in the unification of the mesogastropods and neogastropods into a new group

named Caenogastropoda, which now comprises about 60% of living gastropod species. In terms of rank, Cox (1960) treated Caenogastropoda as an order, while Ponder and Lindberg (1997) (see below) and Bouchet and Rocroi (2005) (see below) treated caenogastropods as an unranked major clade comprising the majority of the Mesogastropoda of Thiele (1929–1931) and all of the Neogastropoda, whilst several groups (Architectonicoidea, Rissoellidae, Omalogyridae, Pyramidellidae, Valvatidae) previously included in Mesogastropoda are now included in Heterobranchia.

Another important change to the old classification was the recognition made by Golikov and Starobogatov (1975) that the true limpets (now described as Patellogastropoda) represent a distinct group from the remaining gastropods. Subsequently, Ponder and Lindberg (1995) grouped the gastropods into two main subclasses: (i) the Eogastropoda, that include the true limpets (Patellogastropoda) and ancestors; and (ii) the Orthogastropoda that are split among the Vetigastropoda, Cocculiniformia, Neritimorpha, Caenogastropoda and Heterobranchia (the latter includes the Opisthobranchia and Pulmonata)(see Figure 4).

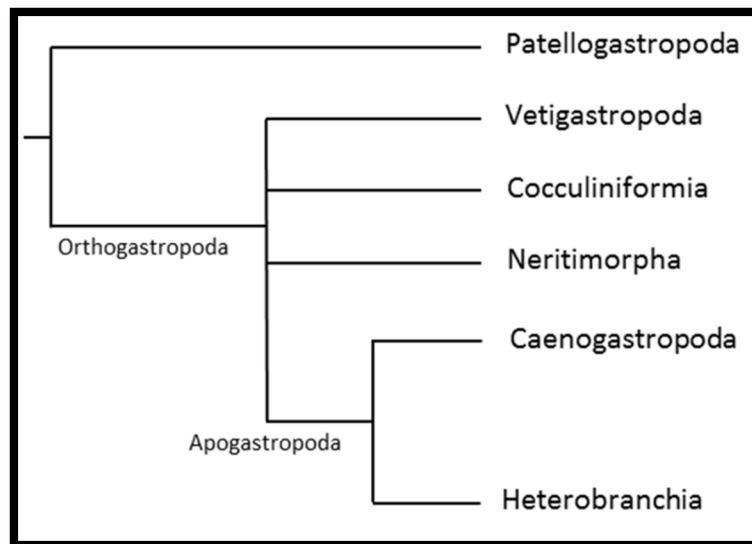


**Figure 4.** Gastropoda classification after Ponder and Lindberg 1995. The class Gastropoda was first divided into two main divisions Eogastropoda (= Patellogastropoda), and Orthogastropoda. Orthogastropoda includes all the other gastropods.

Bouchet and Rocroi (2005) (see Figure 5) recognized the monophyly of the six groups scheme of Ponder and Lindberg (1995) although they consider that there are no synapomorphies that reliably group any of these lineages. These authors proposed slight changes in this systematics, including the elimination of the split between Eogastropoda and Orthogastropoda as in Ponder and Lindberg (1997), and recognizes six main groups: Patellogastropoda, Neritimorpha, Cocculiniformia, Vetigastropoda, Caenogastropoda (which, in the initial classification, all together constituted the subclass Prosobranchia) and Heterobranchia (combining the previous Pulmonata and Opisthobranchia subclasses). In the Bouchet and Rocroi (2005) classification the higher taxa are expressed as unranked clades, and groups where monophyly (a single lineage) is not proved are termed "informal groups".

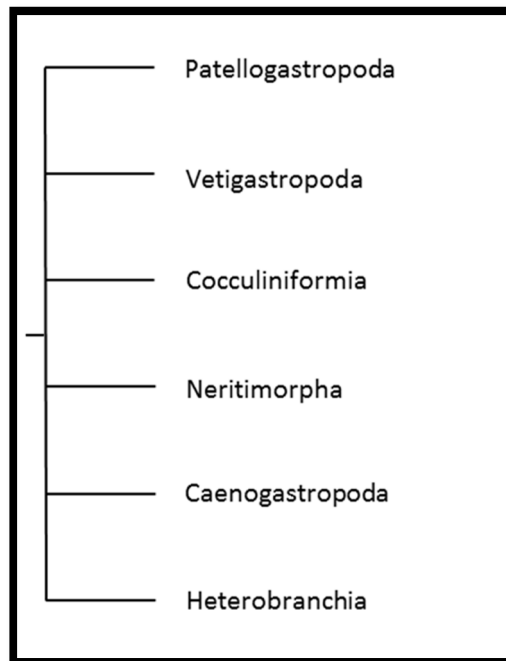


**Figure 5. Gastropoda classification after Bouchet and Rocroi (2005). The class Gastropoda was divided into six monophyletic groups.**

Subsequent revisions by other authors have been made since the publication of the above paper but this dissertation will be based hereafter on the taxonomy proposed by Bouchet and Rocroi (2005), following the adaptations performed by Gofas (2011a) that are adopted in the official site of the *World Register of Marine Species* ([www.marinespecies.org](http://www.marinespecies.org)). Main changes adopted by Gofas (2011a) on the Bouchet and

Rocroi (2005) scheme consisted in adding Linnean ranks above superfamily in order to allow to follow hierarchical levels after a number of branchings and also to better quantify how deep diversification goes (Figures 5 and table 2).

## 2.1.2. Location, structure and function of gastropod statocyst

### 2.1.2.1. Statocyst location

Gastropods statocysts are intimately connected to the nervous system. The nervous system structures, including pedal, pleural and cerebral ganglia, are connected and form a ring around the esophagus (Figure 6).

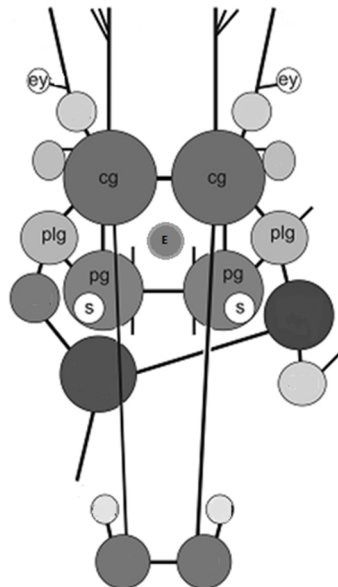


Figure 6. Gastropod central nervous system (schematic dorsal view, not to scale). Cg: cerebral ganglion; E: oesophagus; Ey: eye; Plg: pleural ganglion; Pg: pedal ganglion; S: statocyst. Adapted from Neusser *et al.* 2009.

The statocysts are intimately associated with the nervous ganglia (Fretter and Graham 1962) and frequently connected to the cerebral ganglia through a fine sensory nerve that runs alongside the cerebro-pedal connective nerve (Hyman 1967; Zaitseva 1994; Balaban 2011). The statocyst nerve spreads over the surface of the vesicular wall and presumably terminates in sensory cells (Hyman 1967). The precise location seems to vary from species to species as their description in the literature is rather variable. In infraclass Pulmonata the statocyst is a transparent vesicle that can reach 480  $\mu\text{m}$  and is

located in the cerebro-pedal connective nerves of pedal ganglia (Stahlschmidt and Wolff 1972; Zaitseva and Bocharova 1981; Zaitseva 1994, 2001). However, according to Chase *et al.* (2002) opisthobranchs and pulmonates have the statocysts located on the dorso-lateral surface close to the pleural ganglion, while in the remainder gastropods they are located on the ventral side of the pedal ganglia. The statocyst position in several gastropod species is described in table 1.

**Table 1. Statocyst location in some gastropods species.**

<b>Species</b>	<b>Infraclass or order; Subclass</b>	<b>Statocyst Location</b>	<b>Reference</b>
<i>Patella vulgata</i>	<b>Patellogastropoda</b>	In the cerebro-pedal connective nerve	Fretter and Graham 1962
<i>Pomacea paludosa</i>	unassigned <b>Caenogastropoda</b>	Ventral to the pedal ganglia	Stahlschmidt and Wolf 1972
<i>Ilyanassa obsoleta</i>	Neogastropoda; <b>Caenogastropoda</b>	Close to pedal ganglia	Dickinson and Croll 2003
<i>Aplysia sp.</i>	Opisthobranchia; <b>Heterobranchia</b>	Between the pedal and pleural ganglia	Mckee and Wiederhold 1974; Wiederhold <i>et al.</i> 1989
<i>Pleurobranchaea japonica</i>	Opisthobranchia; <b>Heterobranchia</b>	In the periganglionic connective tissue of pedal ganglia	Ohsuga <i>et al.</i> 2000
<i>Clione limacina</i>	Opisthobranchia; <b>Heterobranchia</b>	On the dorsal surface of the pedal ganglia	Levi <i>et al.</i> 2004
<i>Coryphella rufibranchialis</i>	Nudibranchia; <b>Heterobranchia</b>	Between cerebropleural and pedal ganglia in the short cerebropedal connective	Zaitseva 2001
<i>Lymnaea sp.</i>	Pulmonata; <b>Heterobranchia</b>	Within the pedal ganglia	Sakakibara 2005, 2006

### **2.1.2.2. Statocysts structure**

The statocyst structure is poorly described in class Gastropoda, with the notable exception of Heterobranchia subclass. Statocysts are small spherical organs, filled with

endolymph or statolymph (Mckee and Wiederhold 1974; Hyman 1967). The statocyst wall consists of an outer layer of connective tissue and an inner flattened epithelium (Hyman 1967). The epithelium contains small supporting cells carrying microvilli and giant sensory hair cells (receptor cells) (Fretter and Graham 1962; Stahlschmidt and Wolff 1972; Gao and Wiederhold 1997; Chase 2002; Tsurulis, 1974 in Levi *et al.* 2004). Gastropods can have receptor cells type 1 ("Prosobranchs"), type 2 (Opisthobranchs and Pulmonates) or both types (Opisthobranchs); receptor cells type 1 are morphologically polarized and have the basal feet of the cilia project in the same direction; receptor cells type 2 are morphologically nonpolarized, and the basal feet of the cilia of this hair cell are radially oriented and are most often oriented centripetally with the cilia arranged in a ring (See Salley 1986).

In Opisthobranchia infraclass the statocyst diameter varies with the size of the animal and may reach 200  $\mu\text{m}$  (Wiederhold *et al.* 1989; Ohsuga *et al.* 2000; Zaitseva 2001). Each statocyst contains 10–13 disk-shaped receptor cells (or mechanoreceptor cells (Mckee and Wiederhold 1974; Pedrozo *et al.* 1996)), the number of receptor cells varies from species to species in the Heterobranchia subclass (Ohsuga *et al.* 2000). The receptor cells are separated from each other by layers of small supporting cells (Wiederhold *et al.* 1989; Pedrozo *et al.* 1996; Ohsuga *et al.* 2000; Zaitseva 1994; Zaitseva 2001).

In the caenogastropod *Pomacea paludosa* the statocyst can reach a diameter of 400-450  $\mu\text{m}$  and contain approximately 2500-3000 small receptor cells (Stahlschmidt and Wolff 1972; Gao and Wiederhold 1997). Each receptor cell has 30-40 cilia and is surrounded by 6 supporting cells (Stahlschmidt and Wolff 1972). In gastropods, the receptor cells carry (9+2)-type kinocilia with about 0,2  $\mu\text{m}$  in diameter and 15-20  $\mu\text{m}$  long (Stahlschmidt and Wolff 1972; Mckee and Wiederhold 1974; Gao and Wiederhold 1997; Balaban *et al.* 2011). These cells send their axons into a nerve, called the "static nerve" or statonerve, which connects to the cerebral ganglion (Stahlschmidt and Wolff 1972; Mckee and Wiederhold 1974; Wiederhold *et al.* 1989; Ohsuga *et al.* 2000; Barker 2001; Zaitseva 2001; Chase 2002; Campbell *et al.* 2008). The receptor cells cilia are in direct contact with

the statocyst cavity (Zaitseva 2001). Statocysts contain inside the lumen a single statolith or statoconia (Balaban *et al.* 2011). Upon stimulation of cilia by statoliths or statoconia, there are substances that are activated in specific locations in the statocyst, that function as statocysts sensory transmitters to the cerebral ganglia (see Ohsuga *et al.* 2000; Balaban 2011). Electrophysiological studies conducted by Jance (1988) demonstrated that catecholamines play an important role in the efferent innervation of statocyst by central nervous system neurons (Jance *et al.* 1988 *in* Zaitseva 2001).

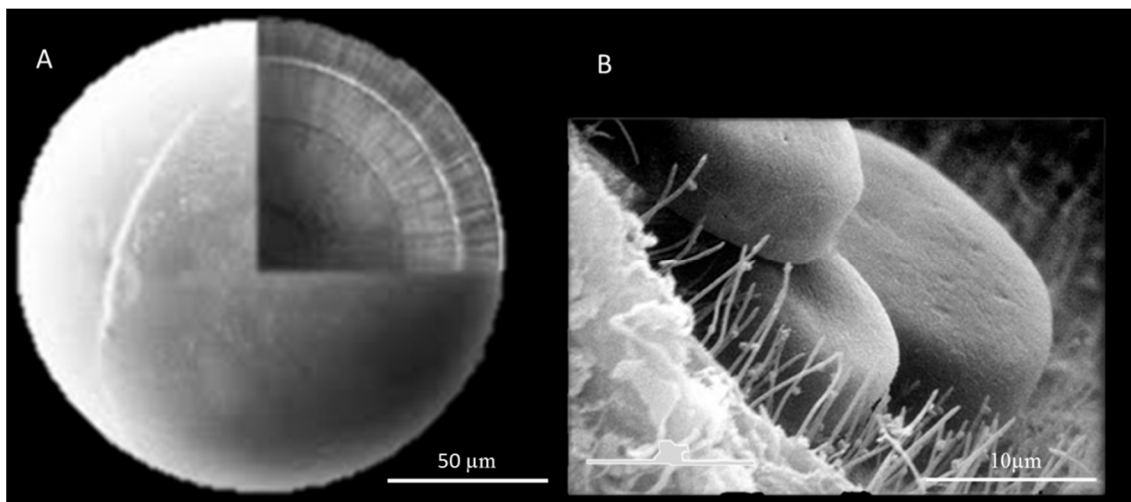


**Figure 7. Statolith and Statoconia. A: Statolith of *Nassarius reticulatus* showing the external appearance and the concentric layers or rings that can be observed when statolith is grinded down to the centre (here represented in just one quarter of the statolith), adapted from Barroso *et al.* 2005. Scale bar 50μm. B: Interior wall of statocyst with three statoconia and several cilia of *Helix lucorum*, extracted from Gorgiladze *et al.* 2010. Scale bar 10 μm.**

The gastropod statolith is generally a spherical mass of calcium carbonate. The statolith is formed by the periodically deposition of increments (Franc 1968) and often shows concentric rings, perhaps due to rhythms in the animal's growth (Fretter and Graham 1962; Maggenti 2005) (see figure 7a). These rings have been used for age estimation in larvae (Grana-Rafucci and Appeldoorn 1997) and adult caenogastropods (Barroso *et al.* 2005, 2011; Richardson *et al.* 2005a, 2005b; Chatzinikolaou and Richardson 2007). The statoconia is constituted by several smaller spherical masses also of calcium carbonate (Figure 7b). Vast majority of statoconia have an ellipsoidal shape in Opisthobranchia infraclass that can vary between 3-20 μm in *Aplysia sp* (Wiederhold *et al.*

1989), and in Pulmonata infraclass have an oval shape structure and can vary between 2-3  $\mu\text{m}$  in diameter (Gorgiladze *et al.* 2010). The statoconia have a central nucleus and the number of layers surrounding it increase with increasing statoconium size (statoconia with an irregular form can have 2 nucleus) (Gorgiladze *et al.* 2010). In *Aplysia* sp., the animals starts with a single statolith (in larval stage) and reaches up to 1000 statoconia in adult life. This indicates that statoconia are added to the cyst lumen during development (Mckee and Wiederhold 1974; Wiederhold *et al.* 1989; Chase 2002).

### **2.1.2.3. Statocysts function**

The statocyst of molluscs was first described as a sense organ, in 1887, by the French zoologist Yves Delage (Franc 1968). Subsequent experimental work carried out by different researchers confirmed that statocysts are organs of balance allowing most of the invertebrates to sense gravity and to maintain the equilibrium (Hyman 1967; Franc 1968; Mckee and Wiederhold 1974; Wierderhold 1989; Gao and Wiederhold 1997; Maggenti 2005; Campbell *et al.* 2008; Gorgiladze *et al.* 2010). Through behavioral experiments, especially statocyst extirpation experiments, it was possible to discover that statocysts of molluscs control various behavioural reactions, like geotaxis (Lever and Genze in Hyman 1967; Levi *et al.* 2004), maintenance of equilibrium (Morton 1979) and compensatory reactions (Barker 2001; Zaitseva 2001; Levi *et al.* 2004). All these findings prove the ability of the statocyst to use gravitational stimuli to spatially orient the body with respect to the vertical axis of gravity (Salley 1986).

Statoliths and statoconia move freely inside the statocyst under the influence of gravity (Mckee and Wiederhold 1974; Levi *et al.*, 2004). Inside the statocyst the continuous beating of the mechanosensory cilia keeps the statoconia in constant motion (Pedrozo *et al.* 1996). Gravity pulls the statoconia down, obstructing the beating of the cilia on the bottom of the statocyst, which causes an increase in membrane conductance to  $\text{Na}^+$  and the formation of an action potential, generating a nervous signal and activating the sensory cells (Wiederhold 1976; Gallin and Wiederhold 1977; Zaitseva 1994; Pedrozo *et al.* 1996; Chase 2002). However, in gastropods, no response is given by

either acceleration or deceleration, and the statocyst only senses the gravity direction (Chase 2002).

In genus *Aplysia* the cerebral ganglia receive information from the statocyst to regulate body movement activity (Salsnki *et al.* cited in Zaitseva 2001). Wiederhold (1989) described that the receptor cells of *Aplysia sp.* statocysts react to a tilted table, generating action potentials. These action potentials are carried by the statocyst nerve to the cerebral ganglia in order to convey information about animal orientation (Gallin and Wiederhold 1977; Wiederhold 1989). It is well established now that the response of receptor cells with respect to gravity is what determines the spatial orientation in gastropods (Gao and Wiederhold 1997). Because of its relatively simple structure, the statocyst of Heterobranchia subclass has been used as a model for zoology studies regarding the basic principles and interactions between the vestibular system and other sensory systems in vertebrates during the formation of adaptive behavior (Zaitseva 2001).

#### **2.1.2.4. Statocyst ontogeny**

The ontogeny and the mechanisms of elemental deposition of gastropods statoliths and statoconia are still poorly known. It is consensual that statocysts are formed very soon during gastropod embryonic development and are functional in the beginning of the larval stage.

Loyd (2008) reported that in the caenogastropod *Kelletia kelletii* the statocysts and respective statoliths are formed approximately within the 2 weeks after egg capsules are laid. D'Asaro (1965) refer that in the caenogastropod *Strombus gigas* statocysts begin to form in "four day old" embryos and are functional by day six. According to Muley (1978), the two statocysts are the most striking features in the trochophore stage (origin of different organs and organ system can be traced from this stage). However, in *N. lapillus* (caenogastropod), the statocysts appears in the beginning of the veliger stage (Muley 1978; Stöckmann-Bosbach 1988; Dickinson and Croll 2003). Then, the statocysts lie close to the pleural-pedal ganglia though they are innervated by nerves from the cerebral

ganglia (Fretter and Graham 1962). In none of these works, on *N. lapillus*, is referred when the statocyst start to develop a statolith.

In the opisthobranch *Aplysia sp.* statocysts arise 10 days after fertilization, when the animals hatch (Wiederhold 1989). However, Bidwell *et al.* (1986) described the presence of a statolith in normal 5 day embryos (Bidwell *et al.* 1986 cited in Wiederhold 1989)

Gorgiladze *et al.* (2010) refer that the statoconia in the pulmonate *Helix lucorum* are formed by deposition of growth layers of mineral and organic materials. These authors found inside the statocyst, apart from statoconia, spherical formations between kinocilia with only 0.3-2.5  $\mu\text{m}$  in diameter that may correspond to the nuclei of future statoconia. Afterwards, the supporting cells secrete the mineral component that sediments in the form of growth layers around the nuclei (Gorgiladze *et al.* 2010).

There are some substances known to be required for the statolith and statoconia production. Pedrozo *et al.* (1996) suggest that urease and carbonic anhydrase are required for statoconia formation and that they are important for regulation of statocyst pH in cultured statocysts (Pedrozo *et al.* 1996). Campbell and Speeg (1969) proposed that ammonia, produced as a consequence of urease activity, can facilitate the biological deposition of calcium carbonate by acting as a proton acceptor (Campbell and Speeg 1969; Pedrozo *et al.* 1996). Strontium is also required to obtain normal development of molluscan statoconia (Wiederhold *et al.* 1989).

The statocysts ontogeny in the opisthobranchs is quite different from other gastropods because in this group larvae presents a single statolith in the statocyst whilst adults possess multiple statoconia (McKee and Wiederhold 1974; Chia *et al.* 1981; Wiederhold 1989; Wiederhold *et al.* 1990). The statolith is retained till the metamorphosis and afterwards statoconia begin to be produced (Wiederhold, 1974; Wiederhold *et al.* 1986). This indicates that statoconia are added to the cyst lumen during development (Wiederhold 1989). Statoconia production reaches the highest level immediately after metamorphosis and then it slows down throughout the rest of animals's life (Wiederhold *et al.* 1990).

## 2.2. Objectives

The main objective of this chapter is to describe the diversity of statoliths and statoconia among several aquatic and terrestrial gastropod species collected in Aveiro (NW Portugal). Besides the general interest in comparing these structures between different species, namely in what regards to their size and external appearance, the ultimate goal is to inspect the clearness of the rings they may possess and their potential interest for sclerochronology studies.

## 2.3. Materials and Methods

### 2.3.1 Statoconia vs statoliths: the diversity within class gastropoda

Samples of marine gastropods were collected by hand in Ria de Aveiro (*Aplysia sp.*, *Calliostoma zizyphinum*, *Crepidula fornicata*, *Gibulla cineraria*, *Gibulla umbilicallis*, *Littorina littorea*, *Monodonta lineata*, *Nassarius incrassatus*, *Nucella lapillus*, *Ocenebra einacea*, *Ocenebrina aciculata*, *Trivia monacha* at Praia da Barra, 40° 31' 05.90" N 8° 47' 05.11" W; *Hydrobia ulvae* at Gafanha da Nazaré 40° 37' 16.43" N 8° 44' 14.69" W) in November 2009, March 2010, and September 2011, during the low tide; species from genus *Helix* terrestrial gastropods were collected in March 2011 in a garden (Santa Joana 40° 37'40.45" N 8 ° 37'25.18" W). *Aporrhais pespelecani*, *Charonia lampas*, *Nassarius reticulatus* and *Ranella olearium* were obtained from the seacoast of Aveiro (10-30 m depth) in sampling surveys performed in 2006 and 2010 preserved frozen (-20°C) thereafter. Specimens were frozen in the following 3-4 hours after collection and kept at -20° till further analysis. Upon thawing, the shells were photographed and measured. The soft body of the animals was extracted from the shell. The anterior ventral surface of the body was dissected under a stereo-microscope to locate the statocysts. The statocysts were gently ruptured and the statoliths were removed with forceps. Statoliths were placed in a supersaturated NaOH solution for 3h. Subsequently, they were washed twice

in distilled water, and then dehydrated, first in ethanol 70% and then in 100%. The statoliths were then mounted in a glass slide with Eukit® resin. The statoliths were photographed under an optical microscope with a microscope camera (Motic 2300®).

### **2.3.2 Statocysts location and structure**

In order to observe the microscopic structure of the statocyst, we selected one gastropod species – *Nassarius reticulatus* - to perform histological preparations of this organ. Specimens were narcotized and afterwards the shells were cracked to remove the soft body. The tissues involving the statocysts were extracted and were fixed in Bouin's solution for 24h. A total of seven pairs of statocysts (obtained from seven animals) were embedded in paraffin, sectioned (7 µm) in a microtome (Leitz 1512, Wetzlar, Germany), stained with haematoxylin–eosin and mounted on a glass slide with EUKIT resin for light microscope observation.

### **2.3.3 Statolith morphology and ontology**

So as to know more about the gastropod statolith ontogeny, one gastropod species *Nucella lapillus* (Linnaeus) was selected. Thus, in the laboratory, the embryonic development of these whelks was followed, from the capsule deposition to juvenile hatching, in order to define the moment when statocysts form and to study the respective morphology of the statolith. For that we collected adults of *N. lapillus* from Praia da Barra and placed them in aquaria with artificial seawater (Prodac®) of 35 practical salinity units (psu), under constant aeration and at 18° C, for female spawning. Every day egg-capsules were removed from the aquaria and kept under the same conditions but separated by date. Once a week, capsules were opened, using a scalpel, and embryonic development was observed with a stereo-microscope and photographed with a digital camera (Moticam® 2300) adapted to the light microscope.

In complement, *N. lapillus* of different sizes were collected in a sheltered beach (Marégrafo, Aveiro) in September 2011 and in an exposed beach (Costa Nova, Aveiro) in November 2011. In the laboratory the shells were measured and the statoliths were

removed from animals and prepared as described above. The statoliths were photographed with the digital camera (Moticam® 2300) adapted to the light microscope and all dimensions measured through image analysis using the Motic Images Plus 2.0® software.

## **2.4. Results and Discussion**

### **2.4.1. Statoconia vs statoliths: the diversity within class gastropoda**

We collected 19 gastropod species from marine, freshwater and terrestrial environment. A wide diversity of taxonomic groups could be sampled, covering 4 subclasses and 13 families: subclass Patellogastropoda (Family Patellidae), subclass Vetigastropoda (Families Calliostomatidae and Trochidae), subclass Caenogastropoda (Families Calyptraeidae, Littorinidae, Hydrobiidae, Aporrhaidae, Ranellidae, Triviidae, Nassariidae and Muricidae,) and subclass Heterobranchia (infraclass Opisthobranchia, family Aplysiidae; infraclass Pulmonata, family Helicidae). The 19 gastropod species collected in this work are shown in figures 8-27 and their taxonomic position is listed in table 2. The taxonomic diversity of gastropods sampled in Aveiro, although relatively short in number of species, is reasonable good to represent the main trends in statocyst diversity in class gastropoda considering that it includes 4 of the main 6 clades of Bouchet and Rocroi (2005).

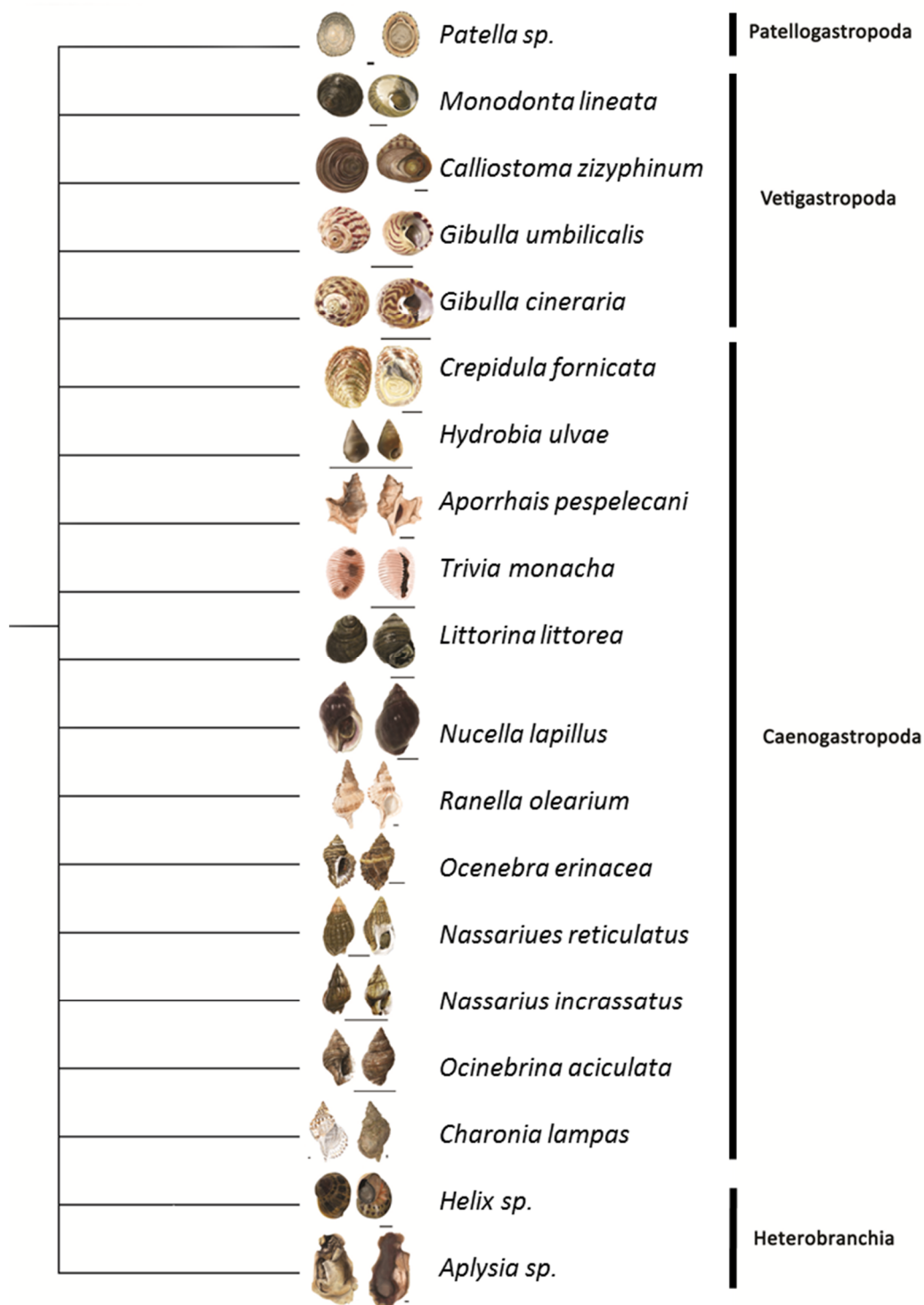


Figure 8. Gastropod tree showing the collected species and their arrangement based on the classification of Bouchet and Rocroi (2005).

## Subclass Patellogastropoda

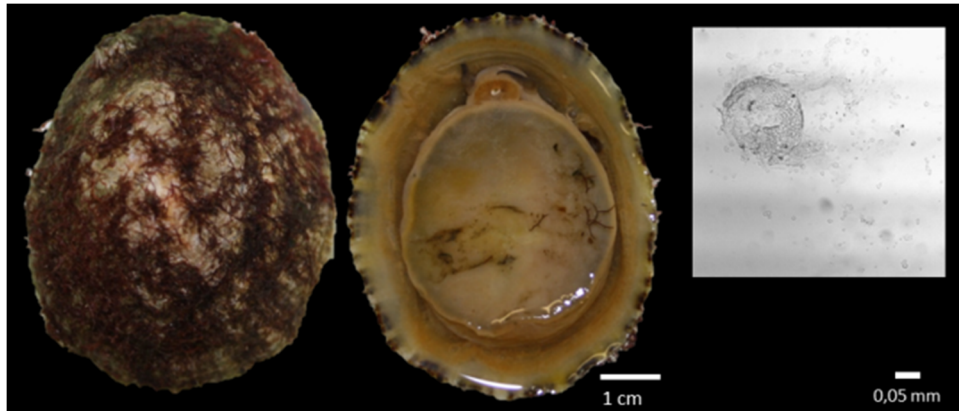


Figure 9. *Patella* sp. From left to right: Shell dorsal view; shell ventral view; Statocyst open and statoconia.

## Subclasse Vetigastropoda

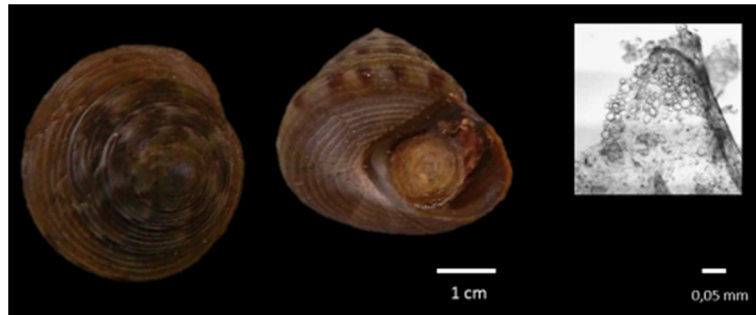


Figure 10. *Calliostoma zizyphinum*. From left to right: Shell apical view; shell apertural view; Statocyst wall and statoconia.



Figure 11. *Gibulla cineraria*. From left to right: Shell dorsal view; shell apertural view; Statoconia.



Figure 12. *Gibulla umbilicallis*. From left to right: Shell dorsal view; shell apertural view; Statocyst with statoconia.



Figure 13. *Osilinus lineatus*. From left to right: Shell dorsal view; shell apertural view; statoconia.

## Subclasse Caenogastropoda



Figure 14. *Aporrhais pespelecani*. From left to right: Shell dorsal view; shell ventral view; Statolith with a central nucleus and 4 rings.



Figure 15. *Charonia lampas*. From left to right: Shell dorsal view; shell ventral view; Statolith with 13 rings.

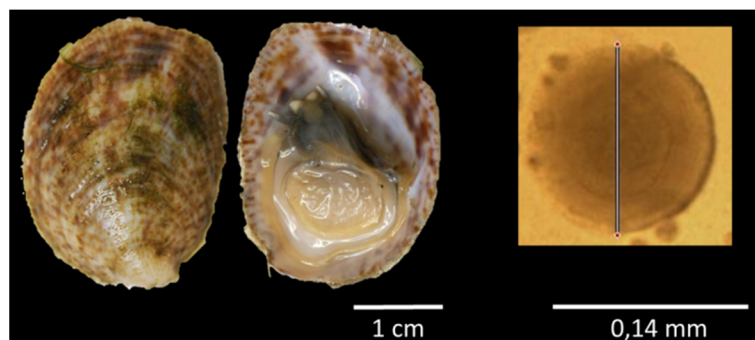


Figure 16. *Crepidula fornicate*. From left to right: Shell dorsal view; shell ventral view; Statolith with 3 rings.

Subclasse Caenogastropoda (cont.)

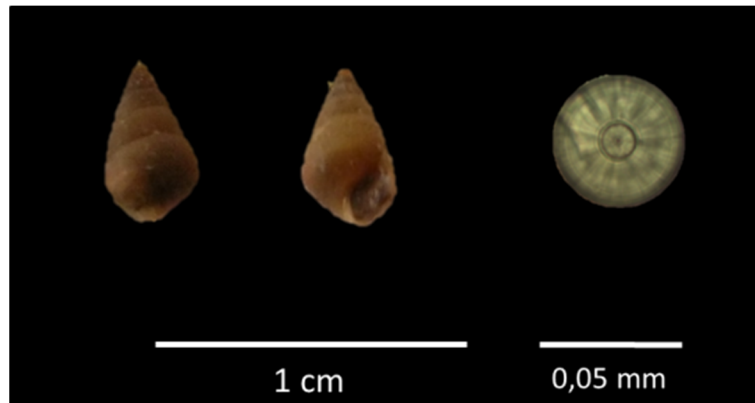


Figure 17. *Hydrobia ulvae*. From left to right: Shell dorsal view; shell ventral view; Statolith with a central nucleus and , metamorphic ring well defined, annual rings not defined.



Figure 18. *Littorina littorea*. From left to right: Shell dorsal view; shell ventral view; Statolith with a central nucleus and several rings.



Figure 19. *Nassarius incrassatus*. From left to right: Shell dorsal view; shell ventral view; Statolith with a central nucleus, metamorphic ring well defined and annual rings not defined.

Subclass Caenogastropoda (cont.)



Figure 20. *Nassarius reticulatus*. From left to right: Shell dorsal view; shell ventral view; Statolith with a central nucleus, metamorphic ring well defined and 4 rings.

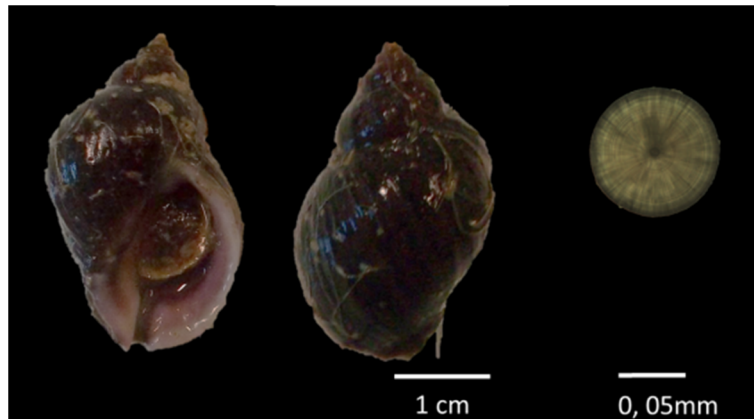


Figure 21. *Nucella lapillus*. From left to right: Shell dorsal view; shell ventral view; Statolith with a central nucleus and annual rings not defined.



Figure 22. *Ocenebra erinacea*. From left to right: Shell dorsal view; shell ventral view; Statolith with a central nucleus and annual rings not defined.

Subclass Caenogastropoda (cont.)

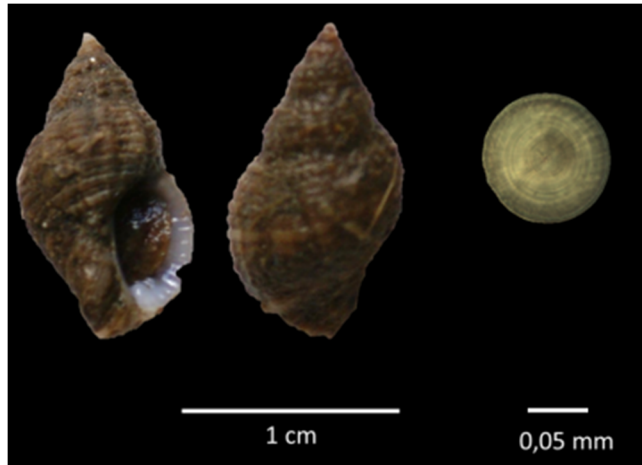


Figure 23. *Ocinebrina aciculata*. From left to right: Shell dorsal view; shell ventral view; Statolith without defined rings.

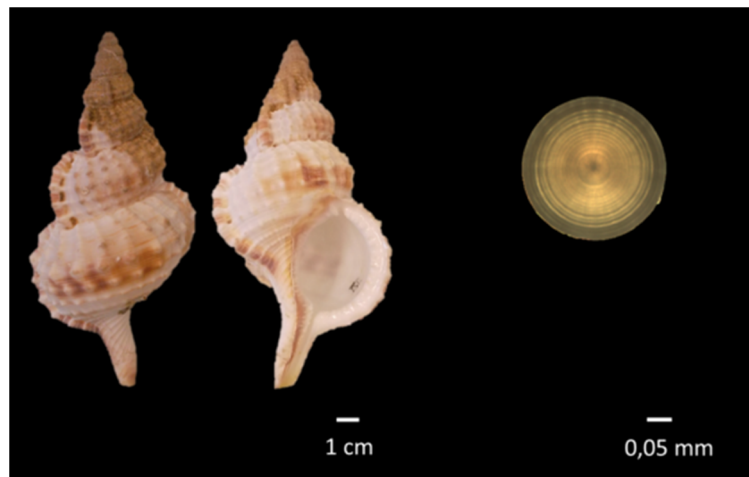


Figure 24. *Ranella olearium*. From left to right: Shell dorsal view; shell ventral view; Statolith with a central nucleus and well defined rings.



Figure 25 *Trivia monacha*. From left to right: Shell dorsal view; shell ventral view; Statolith with a central nucleus and rings not defined.

## Subclass Heterobranchia

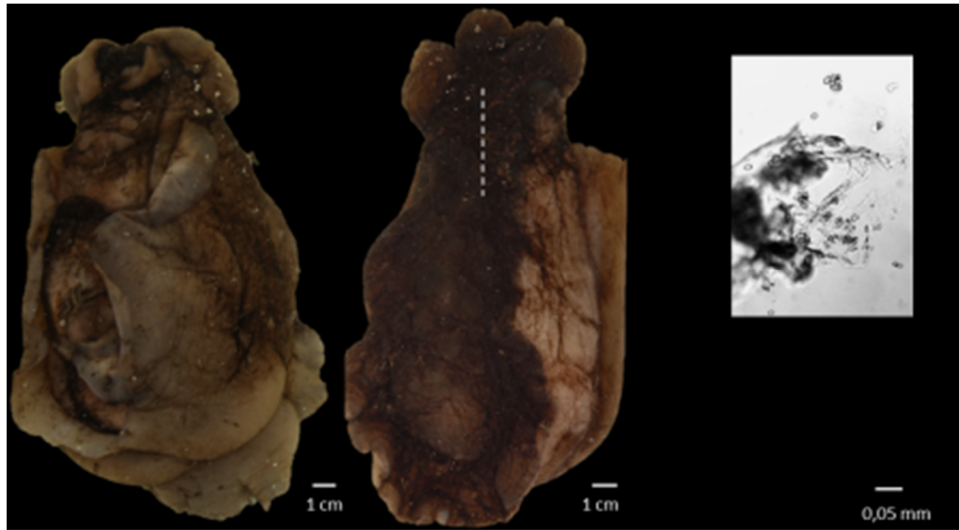


Figure 26. *Aplysia sp.* From left to right: Animal dorsal view; animal ventral view; Statocyst open and statoconia.

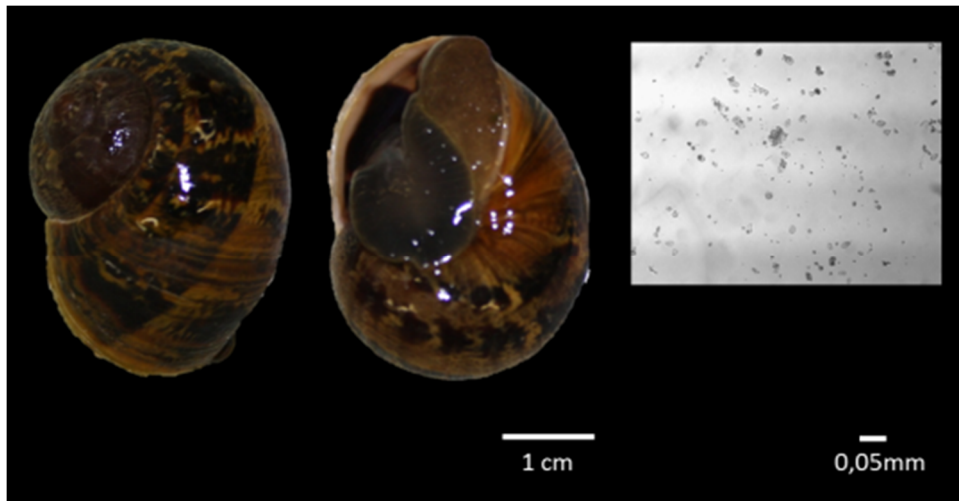


Figure 27. *Helix sp.* From left to right: Shell dorsal view; shell ventral view; statoconia.

Table 2. Taxonomic tree of the species used in the present work. **Statoconia**;  **Statolith**; 

Kingdom Animalia

Phylum Mollusca

Class Gastropoda

Subclass Patellogastropoda

Superfamily Patelloidea

Family Patellidae

Genus *Patella* Linnaeus, 1758 

Subclass Vetigastropoda

Superfamily Trochoidea

Family Trochidae

Subfamily Cantharidinae

Genus *Gibbula*

Species *Gibbula cineraria* Linnaeus, 1758 

Species *Gibbula umbilicalis* da Costa, 1778 

Genus *Osilinus*

Species *Osilinus lineatus* da Costa, 1778 

Family Calliostomatidae

Subfamily Calliostomatinae

Genus *Calliostoma*

Species *Calliostoma zizyphinum* Linnaeus, 1758 

Subclass Caenogastropoda

Order Littorinimorpha

Superfamily Calyptraeoidae

Family Calyptraeidae

Genus *Crepidula*

Species *Crepidula fornicata* Linnaeus, 1758 

Superfamily Littorinoidea

Family Littorinidae

Genus *Littorina*

Species *Littorina littorea* Linnaeus, 1758 

Superfamily Rissoidae

Family Hydrobiidae

Genus *Hydrobia*

Species *Hydrobia ulvae* Pennant, 1777 

Superfamily Stromboidea

Family Aporrhaidae

Genus *Aporrhais*

Species *Aporrhais pespelecani* Linnaeus, 1758 

**Superfamily Tonnoidea**

**Family** Ranellidae

**Subfamily** Ranellinae

**Genus** *Ranella*

**Species** *Ranella olearium* Linnaeus, 1758 

**Subfamily** Cymatiinae

**Genus** *Charonia*

**Species** *Charonia lampas* Linnaeus, 1758 

**Superfamily Velutinoidea**

**Family** Triviidae

**Subfamily** Triviinae

**Genus** *Trivia*

**Species** *Trivia monacha* da Costa, 1778 

**Order Neogastropoda**

**Superfamily Buccinoidea**

**Family** Nassaridae

**Genus** *Nassarius*

**Species** *Nassarius incrassatus* Strøm, 1768 

**Species** *Nassarius reticulatus* Linnaeus, 1758 

**Superfamily Muricoidea**

**Family** Muricidae

**Subfamily** Ocenebrinae

**Genus** *Nucella*

**Species** *Nucella lapillus* Linnaeus, 1758 

**Genus** *Ocenebra*

**Species** *Ocenebra erinaceus* Linnaeus, 1758 

**Genus** *Ocinebrina*

**Species** *Ocinebrina aciculata* Lamarck, 1822 

**Subclass Heterobranchia**

**Infraclass Opisthobranchia**

**Order Anaspidea**

**Superfamily Aplysioidea**

**Family** Aplysiidae

**Genus** *Aplysia* Linnaeus, 1767 

**Infraclass Pulmonata**

**Order Stylommatophora**

**Suborder Sigmuretha**

**Superfamily Helicoidea**

**Family** Helicidae

**Genus** *Helix* Linnaeus, 1758 

This work shows that statoconia occurred in Patellogastropoda, Vetigastropoda and Heterobranchia, while Caenogastropods exhibited a statocyst with a single statolith. This is in good agreement with Fretter and Graham (1962), who stated that species from archaeogastropoda (accepted now as Patellogastropoda, Vetigastropoda and Neritimorpha subclasses), Valvatidae (Heterobranchia subclass) and also Viviparidae (Caenogastropoda subclass) have statoconia, while other mesogastropod and neogastropod families (most belonging now to Caenogastropoda subclass) have a single statolith in each statocyst. It should be noted however that, according to Hess et al. (2008), subclasses Cocculiniforma and Neritimorpha (not analyzed in this work) have a single statolith.

Our findings also match the morphological criteria used to distinguish the hypsogastropoda that, among other diagnostic characters, present a single statolith in each statocyst rather than several statoconia (Ponder and Lindberg 2008). The "hypsogastropoda" was a term introduced by Ponder and Lindberg (1997) to include the "higher caenogastropods" of Healy (1988a), i.e., the great majority of extant caenogastropods (most "mesogastropods" and all neogastropods) or, in other words, all caenogastropods other than architaenioglossans, Cerithioidea, and Campaniloidea. This is in general accordance with the criteria defined by Fretter and Graham (1962) in the sense that these authors also exclude the Viviparidae (architaenioglossans) from the meso- and neogastropods as an exception for the statolith type, i.e., animals that possess statoconia instead of a single statolith.

It seems that the presence of statoconia vs statolith could be used as a main distinguishing feature in gastropods classification. A clearly a distinction between subclasses Patellogastropoda, Vetigastropoda and Heterobranchia, altogether presenting statoconia, and the Caenogastropoda, presenting statoliths, is evident in figure 24. Though useful for systematics, we should avoid making for now any inference regarding the evolution history of statocysts in class gastropoda because it would be surprising to observe statoconia in heterobranchs and statoliths in caenogastropods. In fact, this character (statoconia vs statolith) could represent an important drawback to the hypothesis that consider these two subclasses as sister groups. Although Heterobranchia

has been regarded to be the sister group of Caenogastropoda by many paleontologists, some evidence suggests this may not be true (Ponder and Lindberg 2008). In fact, it has been difficult to construct a robust phylogenetic hypothesis for gastropod evolution as relationships among major gastropod clades vary significantly among analyses based on morphological and molecular data sets (see Aktipis *et al.* 2008). Other interesting aspect is that opisthobranchs show the peculiar feature of exhibiting a single statolith within each statocyst during the larval stage and multiple statoconia afterwards (Wiederhold *et al.* 1990; Chase 2002). Although this aspect deserves more study, we cannot reject the hypothesis that the statolith observed in the larval stage can in fact represent a single statoconium that evolves to a condition of multiple statoconia during ontogeny.

Regardless the usefulness of using the statoconia vs statolith criteria for diagnostic proposals, phylogenetic interpretations or taxonomic rearrangements, one pragmatic conclusion of interest is that only statoliths have potential for sclerochronology and, consequently, only the higher caenogastropods (Hypsogastropoda) are of relevance in this respect. In fact, it does not seem reliable to use each single statoconium to track the passage of time if more and more are being continuously produced throughout gastropod live. In this sense, only the statolith can register a continuous passage of time since the birth of the animal until the moment it stops growing. The remaining shelled gastropods can still be used for sclerochronology studies but only through the use of their shells.

#### **2.4.2. Statocysts location and structure**

The statocysts are transparent organs and it is possible to see where they are located due to the distinct presence of the statoliths or statoconia. The gastropods analysed presented statocysts close to the nervous ganglia but, as expected, in different positions depending on the species. For instance, in *N. reticulatus* (see figure 28) statocysts are close to the pedal ganglia, while in *Patella sp*, *C. zizyphinum* and *Aplysia sp* (see Figure 29, 30 and 31, respectively ) statocysts are between the pedal and the pleural ganglia, but closer to the pedal ganglia. In *Helix sp* statocysts are located on the side of the pedal ganglia (Figure 32).



Figure 28. *Nassarius reticulatus*. From left to right: shell dorsal view; shell ventral view; animal without shell (the dotted white line indicates the location of the incision); statocysts close to pleural ganglia.

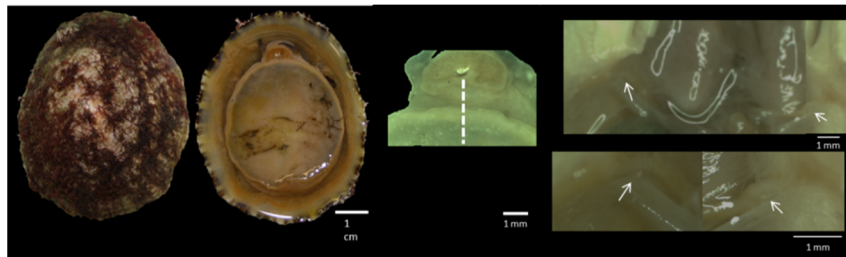


Figure 29. *Patella* sp. From left to right: Shell dorsal view. Shell ventral view. Animal head (the dotted white line indicates the location of the incision); Statocysts between pleural and pedal ganglia, see arrows.

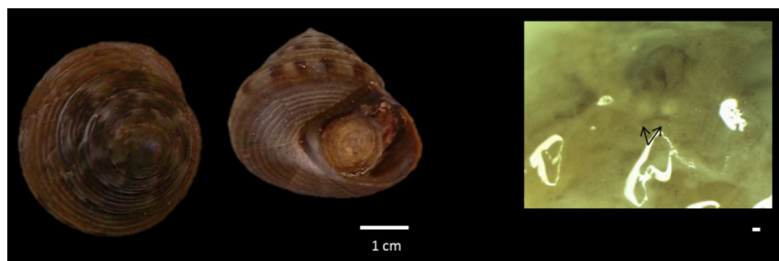


Figure 30. *Calliostoma zizyphinum*. From left to right: Shell dorsal view. Shell ventral view. Statocysts between pleural and pedal ganglia, see arrows.

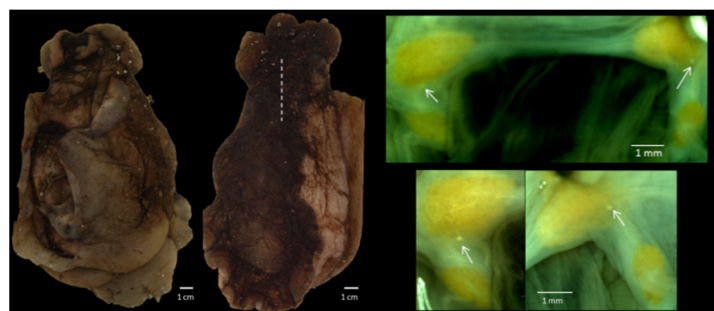


Figure 31. *Aplysia* sp. From left to right: animal dorsal view. Animal ventral view (the dotted white line indicates the location of the incision); Statocysts between pleural and pedal ganglia, see arrows.



Figure 32. *Helix* sp. From left to right: Shell dorsal view. Shell ventral view. Animal without shell (the dotted white line indicates the location of the incision); Pleural-pedal ganglia.

The histology of the statocysts in *N. reticulatus* (Caenogastropoda) did not allow an adequate identification of the cells that constitute the statocyst. In fact, it is possible to observe two cells layers, in the interior of the cyst (Figure 33a and 33b), but it is not possible to identify the cells types (receptor and supporting cells) nor the cilia. Figure 30a shows the *N. reticulatus* statocyst without the statolith as it was removed by the microtome knife during cutting. The *N. reticulatus* statocyst with a statolith is shown in figure 30b. This statolith has been cut and this is just a part (less than a half) of the statolith. A statocyst with a statolith in figure 33c, but in this case a fresh unfixed and unstained preparation was made and photographed immediately after extraction from the animal where it can be observed the round structure and the transparency of the statocyst.

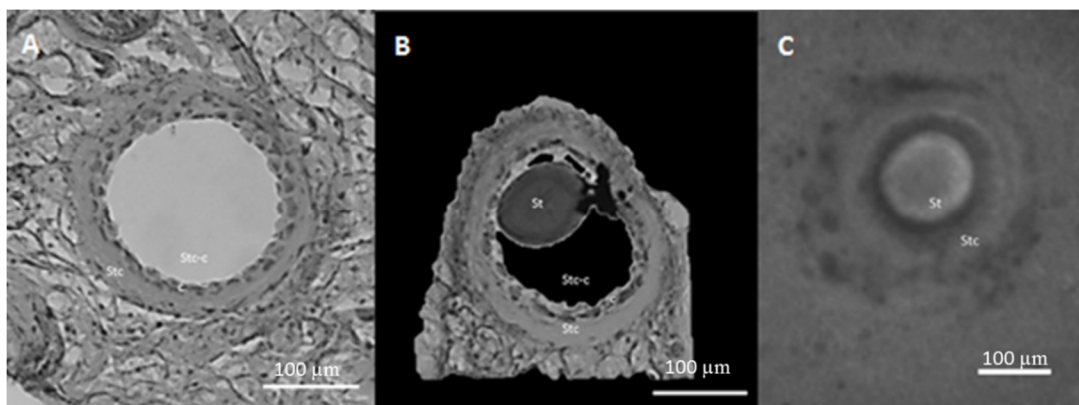


Figure 33. *Nassarius reticulatus*. Histological preparations: statocyst without statolith (A); Statocyst with a statolith (B). A and B: The cells, in the inner of the statocyst, are probably the receptor cells. C: Statocyst in vivo. Statocyst with a statolith. Stc: Statocyst outer wall; Stac-c: Statocyst cavity; c: statocyst inner wall; St: statolith. Scale 100µm.

### 2.4.3. Statolith morphology and ontology

As shown in figures 15-25 the morphology of statoliths is quite similar among the different species of Caenogastropoda. All of them have a more or less spherical shape and exhibit a hard translucent structure. As they are transparent it is possible to perceive the existence of several concentric layers of material that seems to be secreted with a given pattern during the animal's live. These concentric layers are noticed in almost all statoliths (Figures 14-25) and, when observed in one dimension, they appear like a series of rings that can putatively result from a discontinuous growth rate of the animal. Between these conspicuous major rings it is possible to observe other tiny and smaller rings that apparently are formed by progressive deposition of calcareous and organic material during growth. If any of these rings result from annual, monthly, fortnightly or even daily increments of time induced by environmental and astronomical pacemakers, it is possible to use them to trace the passage of time, and here resides their potential value for sclerochronology.

In order to better understand the growth and morphology evolution of the statolith, we followed the statolith development in one selected caenogastropod - *N. lapillus* – during the larval stage (retained in the egg capsule) and in adult live. *N. lapillus* is a predatory gastropod abundant and widespread on rocky shores in the North Atlantic. *N. lapillus* is dioecious, laying benthic capsules that each contains 15–30 shelled embryos. Crawling young emerge from the capsules and, as in other gastropods with direct development, the limited dispersal capability is correlated with pronounced spatial variability in shell morphology (Rolán *et al.* 2004; Guerra-Varela *et al.* 2009; Galante-Oliveira *et al.* 2011).

It has been reported that the period between egg capsule deposition and juvenile hatching in this species may last about 4 months (Fretter and Graham 1962; Stöckmann-Bosbach 1988; Pechenik *et al.* 1984). The embryos were observed once a week, but only in the 3<sup>rd</sup> week (after egg-capsule deposition) was possible to observe the statolith (Figure

34d). It was not possible to distinguish the organs that have developed in the embryos between the first and second week (Figure 34a and 34b, respectively) by direct microscope observation. In the 3<sup>rd</sup> week the statolith presented 3 rings (Figure 34d), which indicates that it was formed some time before, perhaps in the beginning of the second week. This has been confirmed for other caenogastropod, *Kelletia kelletii* (Loyd *et al.* 2008).

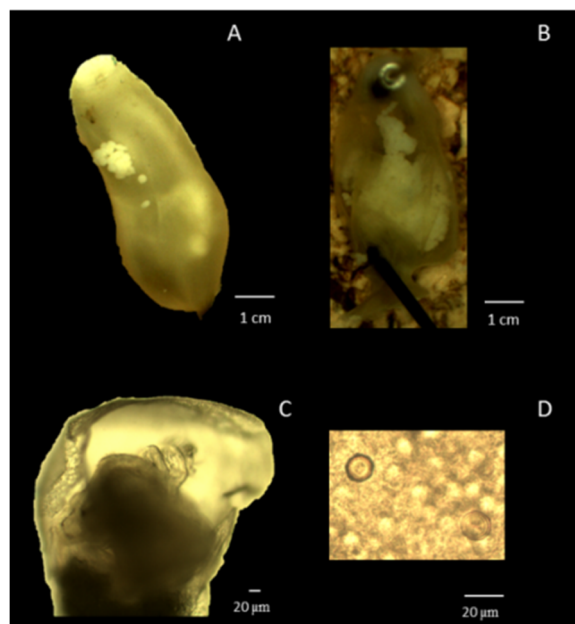


**Figure 34.** *Nucella lapillus* ontogeny. A: Capsule with embryos in the first day. B: Capsule with embryos in the beginning of 2<sup>nd</sup> week. C: Embryo in the veliger stage. D: statolith of an embryo with 24 days.

The monitoring of the continuous development of the statolith beyond the juvenile stage and up to the adult live would take a number of years, so we decided to analyze statoliths from a wide range of animal sizes in order to cover different ages. By this way it was possible to follow the growth of the animals (along the different cohorts) at both sampling sites (Marégrafo and Costa Nova), although the age could not be estimated. *N. lapillus* is known by presenting a polymorphism associated with the degree of wave exposure: exposed ecotypes are typically small, with relatively larger apertures and thinner shells than the sheltered ecotypes. In some localities the sheltered/exposed polymorphism reaches its maximum distinctness in sub-adults and then decreases with

ageing, probably because adults undergo shell erosion (Rolán et al.2004; Guerra-Varela et al. 2009). Despite the specific ecotype of this specie, no difference was found in the statolith between animals in these sites (Marégrafo and Costa Nova). We conclude that the morphology and external appearance of the statolith remained almost constant throughout the live of the whelks in what regards to the shape and occurrence of rings. The diameter of the statoliths increased with shell size (see figure 35) and the number of rings augmented proportionally. The same pattern was already reported for *N. reticulatus* collected from Aveiro by Barroso *et al.* (2005). This result confirms that the statolith increment follows the growth of the animal throughout life and may probably provide an important register of physical and chemical characteristics of the marine environment throughout ontogeny. They could thus serve as a tool for age estimation in *N. lapillus* as well as a possible archive of the environmental conditions that the whelks experienced through lifespan at a given site.

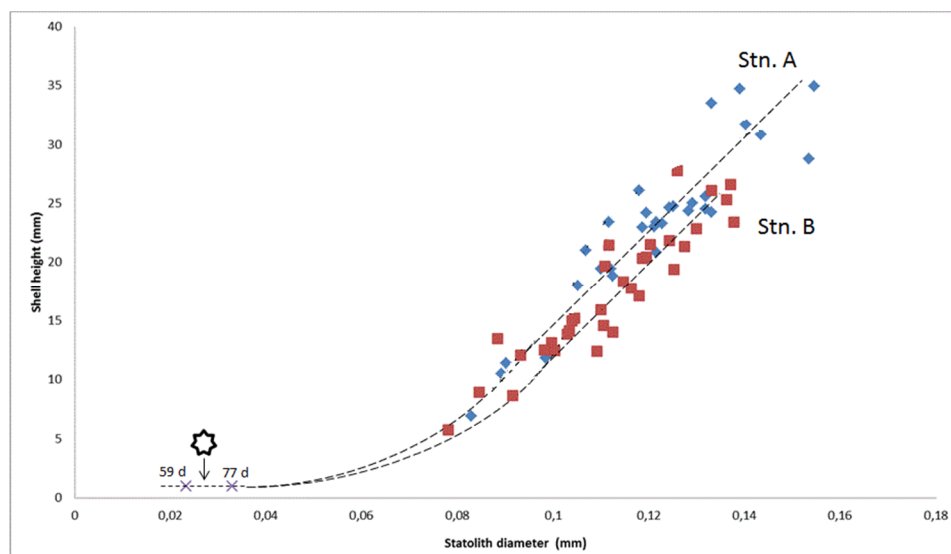


**Figure 35** *Nucella lapillus*. Stn.A: Marégrafo. Stn.B: Costa Nova. The two first points indicates the statolith size with 59 and 77 day of life. The line was adjusted visually and may not represent the real trend between the left (early development inside capsules) and right points (animals collected in the field). (\*) indicates the time to hatch (approx. on 65<sup>th</sup> day).

The statoliths of the diverse caenogastropods species collected in Ria de Aveiro appear to have the potential to be used in sclerochronology studies as: (i) they are easy to

collect; (ii) they grow along the animals life and form in the beginning of ontogeny; and (iii) they present a hard structure that may register the history of the animal throughout time. It is particularly interesting to note that they present rings that could be used to estimate the age of animals if they are produced with a given periodicity. For instance, if each ring observed in the statolith corresponds to the change of growth rate during every winter, their count could easily indicate the age of the gastropods in years. Most importantly, when the statolith is grinded to the centre it reminds a "music CD". If any analytical technique could analyse the chemical composition of the statolith along the radius (from the center to the edge) perhaps we could detect and validate the number of rings if they correspond to seasonal variation of growth and confirm age. If bioaccumulation rate is taken into account it could be even possible to trace temporal evolution of environmental levels of given contaminants at a given site, which would represent a milestone to environmental monitoring science. Hence, after this preliminary approach to understand the diversity and general characteristics of statocysts and statoliths in class gastropoda, it is important to advance and explore new techniques that could allow the chemical analysis of the gastropod statolith, which is the subject of the next chapter.

## 2.5 References

- Aktipis, S. W., Giribet, G., Lindberg, D. R., and Ponder, W. F. (2008). Gastropod Phylogeny: an overview and analysis. In *Phylogeny and Evolution of the Mollusca*. D. R. Lindberg and W. F. Ponder. Berkeley, CA: Berkeley University Press: 201-237.
- Balaban, P. B., P. M., A. Y. Malyshev, *et al.* (2011). Functional Changes in the Snail Statocyst System Elicited by Microgravity. *Plos one* 6(3).
- Barker, G. M. (2001). *The Biology of Terrestrial Molluscs*. New Zealand, CABI.
- Barroso, C. M., M. Nunes, *et al.* (2005). The gastropod statolith: a tool for determining the age of *Nassarius reticulatus*. *Marine Biology* 146(6): 1139-1144.
- Barroso, C. M., Rato, M., Veríssimo, A., Sousa, A., Santos, J. A., Coelho, S., Gaspar, M. B., Maia, F., Galante-Oliveira, S. (2011). Combined use of *Nassarius reticulatus* imposex and statolith age determination for tracking temporal evolution of TBT pollution in the NW Portuguese continental shelf. *Journal of Environmental Monitoring* 13: 3018.
- Bouchet and Rocroi (2005). Classification and nomenclature of gastropod families. *Malacologia* 47 (1-2): 1-397.
- Campbell, J.W. and Speeg, K.V. (1969). Ammonia and the biological deposition of calcium carbonate. *Nature* 224: 725-726.
- Campbell, N., Reece, J., Urry, L., Cain, M., Wasserman, S., Minorsky, P., Jackson, R., Ed. (2008). *Biology*. San Francisco, Pearson Benjamin Cummings.
- Chase, R. (2002). *Behaviour and Its Neural Control in Gastropods Molluscs*. New York, Oxford University Press.
- Chatzinikolaou, E. and Richardson, C. A (2007). Evaluating growth and age of netted whelk *Nassarius reticulatus* (Gastropoda: Nassariidae) using statolith growth rings. *Marine Ecology-Progress Series* 342:163-176.
- Chia, F. S. and Koss, R. (1978). Development and Metamorphosis of the Planktotrophic Larvae of *Rostanga pulchra* (Mollusca: Nudibranchia). *Marine Biology* 46: 109-119.
- Chia, F. S., Koss, R., Bickell, L. R. (1981). "Fine Structural Study of the Statocysts in the Veliger Larva of the Nudibranch, *Rostanga pulchra*". *Cell and Tissue Research* 214:67-80.
- Cox, L. R. (1960). thoughts on the classification of the Gastropoda. *Proceedings of the Malacological Society of London* 33: 239-261.
- D'asaro, C. N. (1965). Organogenesis, development, and metamorphosis in the queen conch, *Stombus gigas*, with notes on breeding habits. Msc Thesis.
- Dickinson, A. J. G. and Croll, R.P.(2003). Development of the Larval Nervous System of the Gastropod *Ilyanassa obsoleta*. *The Journal of comparative neurology* 466:197-218.
- Franc, A. (1968). *Mollusques Gastéropodes et scaphopodes*. Paris, Masson and Cie.

- Fretter, V. and A. Graham (1962). British Prosobranch Molluscs. London, Bartholomew Press.
- Galante-Oliveira, S., Marçal, R., Pacheco, M., Barroso, C. M. (2011). *Nucella lapillus* ecotypes at the southern distribution limit in Europe: variation in shell morphology is not correlated with chromosome counts on the Portuguese Atlantic coast. *Journal of Molluscan Studies* 0: 1–4.
- Gallin, E. K. and Wiederhold, M. L. (1977). Response of *Aplysia* statocyst receptor cells to physiologic stimulation. *Journal of Physiology* 266: 123-137.
- Gao, W., Wiederhold, M. L. (1997). The structure of the statocyst of the freshwater snail *Biomphalaria glabrata* (Pulmonata, Basommatophora). *Hearing research* 109: 109-124.
- Gofas, S. (2011). Gastropoda. Accessed through: World Register of Marine Species at <http://www.marinespecies.org/aphia.php?p=taxdetails&id=101> on 2011-12-1.
- Golikov, A. N., Starobogatov, Y. I. (1975). Systematics of prosobranch gastropods. *Malacologia* 15 (1): 185-232.
- Gorgiladze, G. I., Bukia, R. D., Davitashvili, M. T., Taktakishvili, A. D., Gelashvili, N. Sh., Kalandarishvili, E. L., Satdykova, G. P. (2010). Morphological Peculiarities of Statocyst Statocyst in Statocysts of Terrestrial Pulmonary Snail *Helix Lucorum*. *Bulletin of Experimental Biology and Medicine: Morphology and Pathomorphology* 149:2.
- Grana-Rafucci, F. A. and Appeldoorn, R. S. (1997). Age determination of larval strombid gastropods by means of growth increment counts in statoliths. *Fishery Bulletin* 95:857-862.
- Guerra-Varela, J., Colson, I., Backeljau, T., Breugelmans, K., Hughes, R. N., Rolán-Alvarez, E. (2009). The evolutionary mechanism maintaining shell shape and molecular differentiation between two ecotypes of the dogwhelk *Nucella lapillus*. *Evolutionary Ecology* 23:261–280.
- Hess, M., F. Beck, *et al.* (2008). Microanatomy, Shell Structure and Molecular Phylogeny of *Leptogyra*, *Xyleptogyra* and *Leptogyropsis* (Gastropoda: Neomphalida: Melanodrymiidae) from Sunken Wood. *Journal of Molluscan Studies* 74: 383-401.
- Hyman, L. H. (1967). Mollusca I. New York, McGraw-Hill Book Company.
- Levi, R., Varona, P., Arshavsky, Y. I., Rabinovich, M. I., Selverston, A. I. (2004). Dual Sensory-Motor Function for a Molluscan Statocyst Network. *Journal of Neurophysiology* 91: 336–345.
- Lloyd, D. C., Zacherl, D. C., Walker, S., Paradis, G., Sheehy, M., Warner, R. R. (2008). Egg source, temperature and culture seawater affect elemental signature in *Kelletia kelletii* larval statoliths. *Marine Ecology Progress Series* 353: 115–130.
- Maggenti, M., Maggenti, A. (2005). Online Dictionary of Invertebrate Zoology. S. Gardner. Lincoln, Nebraska.
- Mckee, A. E. and Wiederhold, M. L. (1974). *Aplysia* statocyst receptor cells: fine structure. *Brain research*, 81: 310-313.
- Morton, J. E. (1979). Molluscs. London, Hutchinson & Co. Ltd.
- Muley, E. V. (1978). Embryology and Development of a Freshwater Prosobranch, *Melania-Scabra*. *Hydrobiologia* 58(1): 89-92.

- Neusser, T. P, Hess, M., Schrödl, M. (2009). Tiny but complex - interactive 3D visualization of the interstitial acochlidian gastropod *Pseudunela cornuta* (Challis, 1970). *Frontiers in Zoology*, 6:20.
- Ohsuga, K., Kurokawa, M., Kuwasawa, K. (2000). Mosaic arrangement of SCPb-, FMRFamide- and histamine-like immunoreactive sensory hair cells in the statocyst of the gastropod mollusk *Pleurobranchia japonica*. *Cell and Tissue Research*, 300: 165-172.
- Pechenik, J. A., S. C. Chang, *et al.* (1984). Encapsulated Development of the Marine Prosobranch Gastropod *Nucella-Lapillus*. *Marine Biology* 78(2): 223-229.
- Pedrozo, H. A., Schwartz, Z., Luther, M., Dean, D. D., Boyan, B. D., Wiederhold, M. L. (1996). A mechanism of adaptation to hypergravity in the statocyst of *Aplysia californica*. *Hearing Research* 102: 51-62
- Ponder and Lindberg (1997). Towards a phylogeny of gastropod molluscs: an analysis using morphological characters. *Zoological Journal of the Linnean Society* 119: 83-265.
- Richardson, C. A., P. R. Kingsley-Smith, *et al.* (2005a). Age and growth of the naticid gastropod *Polinices pulchellus* (Gastropoda : Naticidae) based on length frequency analysis and statolith growth rings. *Marine Biology* 148(2): 319-326.
- Richardson, C. A., Saurel, C., Barroso, C. M., Thain, J. (2005b). Evaluation of the age of the red whelk *Neptunea antiqua* using statoliths, opercula and element ratios in the shell. *Journal of Experimental Marine Biology and Ecology* 325:55 – 64.
- Rolán, E., Guerra-Varela, J., Colson, I., Hughes, R. N., Rolán-Alvarez, E. (2004). Morphological and genetic analysis of two sympatric morphs of the dogwhelk *nucella lapillus* (gastropoda: muricidae) from galicia (northwestern spain). *Journal of Molluscan Studies* 70: 179–185
- Sakakibara, M. (2006). Comparative Study of Visuo-Vestibular Conditioning in *Lymnaea stagnalis*. *The Biological Bulletin* 210: 298 –307.
- Sakakibara, M., Aritaka, T. (2005). Electrophysiological responses to light of neurons in the eye and statocyst of *Lymnaea stagnalis*. *Journal of Neurophysiology* 93(1): 493-507.
- Salley, S. (1986) Development of the Statocyst of the Queen Conch larva, *Strombus gigas* L. (Gastropoda: Prosobranchia). Institute of Oceanography, Faculty of Graduate Studies and Research, Montreal, Canada.
- Stahlschmidt, V. and Wolff, H. G. (1972). The Fine Structure of the Statocyst of the Prosobranch Mollusc *Pomacea paludosa*. *Z. Zellforsch* 133: 529—537.
- Stöckmann-bosbach, R. (1988). Early stages of the encapsulated development of *Nucella lapillus* (Linnaeus) (gastropoda, muricidae). *Journal of Molluscan Studies* 54: 181-196.
- Wiederhold, M. L., Sharma, J. S., Driscoll, B. P., Jeffrey, L. (1990). Development of the statocyst in *Aplysia californica*. I. Observations on statoconial development. *Hearing Research* 49: 63-78
- Wiederhold, M. L., Sheridan, C. E., Smith, N. K. R. (1989). Function of molluscan statocyst. Origin, Evolution, and Modern Aspects of Biomineralization in Plants and Animals Edited by Rex E. Crick Plenum Press, New York, 393-408.

- Yonge's (1947) The pallial organs in the aspidobranch Gastropoda and their evolution throughout the Mollusca. Philosophical transactions of the Royal society of London B 232: 443-518.
- Zaitseva, O. V. (1994). Structural organization of the sensory systems of the snail. Neuroscience Behaviour Physiology 24(1): 47-57.
- Zaitseva, O. V. (2001). The Structural Organization of the Statocyst Sensory System in Nudibranch Molluscs. Neuroscience and Behavioral Physiology 31:1.
- Zaitseva, O. V. and Bocharova, L. S. (1981). Sensory cells in the head skin of pond snails. Fine structure of sensory endings. Cell and Tissue Research 220:797-807.



## Chapter 3 - The gastropod statolith chemical composition

### 3.1. Introduction

Statoliths are diverse amongst the Gastropoda class, namely regarding type, shape and microstructure, see chapter 2. These features have been addressed over time, mainly as part of studies on statocysts structure (e.g. McKee and Wiederhold 1974; Chia *et al.* 1981; Gao and Wiederhold 1997; Gorgiladze *et al.* 2010), development (e.g. D'Asaro 1965; Salley 1986; Wiederhold *et al.* 1990; Gao *et al.* 1997) and function (e.g. McKee and Wiederhold 1974; Gallin and Wiederhold 1977; Wiederhold *et al.* 1989). However, the scenario is different regarding statoliths chemical composition and hardly any reports, specifically on gastropods, can be found in the literature.

### 3.2. The gastropod statolith mineral matrix

There are few studies on gastropods statoliths chemical composition and the available ones refer to a minority of species – statoconia in *Helix lucorum* (Gorgiladze 2002) and *Aplysia californica* (Wiederhold *et al.* 1989; Pedrozo *et al.* 1997) – and mostly in larvae – statoliths in *Strombus gigas* (Salley 1986), *Concholepas concholepas* (Zacherl *et al.* 2003a) and *Kelletia kelletii* (Zacherl *et al.* 2003b; Zacherl 2005; Lloyd *et al.* 2008). Generally, a mineral matrix of calcium carbonate ( $\text{CaCO}_3$ ) is referred for both statoconia and statoliths but its crystalline form as aragonite was only effectively tested for *Helix lucorum* (Gorgiladze 2002) and *Aplysia californica* (Pedrozo *et al.* 1997), both species presenting statoconia in adult life. However, embryonic and pre-metamorphic *Aplysia* contain a single statolith within each statocyst, evolving to statoconia during juvenile stage (Wiederhold *et al.* 1990). In this particular case, Pedrozo and co-authors (1997) showed that statolith and statoconia differ regarding crystalline composition: statoconia were proved to be aragonitic while statoliths were apparently of amorphous  $\text{CaCO}_3$ . Despite this unique record, the assumption of an aragonitic matrix in statoliths is patent (Grana-Raffucci and Appeldoorn 1997; Zacherl *et al.* 2003a; Zacherl *et al.* 2003b; Zacherl

2005; Lloyd *et al.* 2008) possibly because the data on statoconia are on that direction (Pedrozo *et al.* 1997; Gorgiladze 2002) but also since detailed descriptions on the chemical composition of analogous structures are available in the literature and show the presence of aragonite crystals (For cephalopod statoliths composition see Radtke 1983; see the comprehensive revision on fish otoliths by Campana 1999).

Regarding elemental composition, the gastropod statolith is known to be dominated by the major chemical elements calcium (Ca), carbon (C) and oxygen (O) (Wiederhold *et al.* 1989; Pedrozo *et al.* 1997; Gorgiladze 2002; Barroso *et al.* 2005b), as expected because of the CaCO<sub>3</sub> matrix. Nevertheless, the presence of minor (>100ppm) and trace (<100ppm) elements have been plainly reported for *Aplysia californica* (Wiederhold *et al.* 1989), *Helix lucorum* (Gorgiladze 2002), *Strombus gigas* (Salley 1986), *Concholepas concholepas* (Zacherl *et al.* 2003a) and *Kelletia kelletii* (Zacherl *et al.* 2003b; Zacherl 2005; Lloyd *et al.* 2008), (see Table 3).

**Table 3. Summary of the records found in literature for minor and trace elements detected in statoconia and statoliths. Elements are presented by species and respective references are also indicated.**

<b>Species</b>	<b>Elements</b>	<b>References</b>
<i>Aplysia californica</i>	Cl, Mg, Na, Sr, S	Wiederhold <i>et al.</i> (1989)
<i>Helix lucorum</i>	Cl, K, Si, Na, S	Gorgiladze (2002)
<i>Strombus gigas</i>	Cl, Mg, Na, P, S	Salley (1986)
<i>Concholepas concholepas</i>	Ba/Ca, Pb/Ca, Sr/Ca, Zn/Ca	Zacherl <i>et al.</i> (2003a)
<i>Kelletia kelletii</i>	Ba/Ca, Sr/Ca	Zacherl <i>et al.</i> (2003b)
	Ba/Ca, Ce/Ca, Mg/Ca, Mn/ Ca, Pb/Ca, Sr/Ca, Zn/Ca	Zacherl (2005)
	Ba/Ca, Mg/Ca, Mn/Ca, Pb/Ca, Sr/Ca, Zn/Ca	Lloyd <i>et al.</i> (2008)

Small but significant amounts of chlorine (Cl), magnesium (Mg), sodium (Na), strontium (Sr) and sulfur (S) were reported as minor elements of *A. californica* statoconia by Wiederhold *et al.* (1989); no absolute values are indicated but the authors determined a Ca/Sr ratio of  $97:1 \pm 3$  (mean  $\pm$  standard error). Chlorine, potassium (K), Na, S and silicon (Si) ranged from 0.1 to 0.7% of the total weight fractions (1000 to 7000 ppm) in *H. lucorum* statoconia (Gorgiladze 2002). Chlorine, Mg, Na, phosphorous (P) and S were also detected in the inner matrix of a 0-10 days larval statolith of *S. gigas* (Salley 1986). Zacherl *et al.* (2003a) measured barium (Ba), lead (Pb), Sr and zinc (Zn) in *Concholepas concholepas* larva, presenting the results as element/Ca ratios, as it was also performed for *Kelletia kelletii* larva by: (i) Zacherl *et al.* (2003b) for Ba/Ca and Sr/Ca ratios; (ii) Zacherl (2005) for Ba/Ca, cerium (Ce)/Ca, Mg/Ca, manganese (Mn)/Ca, Pb/Ca, Sr/Ca and Zn/Ca; and (iii) Lloyd *et al.* (2008) for Ba/Ca, Mg/Ca, Mn/Ca, Pb/Ca, Sr/Ca and Zn/Ca. Thus, in summary and to date, the following elements were detected in gastropods statoconia and statoliths: Ba, C, Ca, Ce, Cl, K, Mg, Mn, Na, O, P, Pb, S, Si, Sr and Zn.

### 3.3. Objectives

The objective of this chapter is to characterize *Nassarius reticulatus* statolith elemental composition by using the Electron Probe Microanalysis (EPMA) technique. EMPA is a non-destructive approach for determining the chemical composition of complex solid materials (Castaing 1960) and proved to be the best method to accurately measure the most representative elements in fish otoliths (Campana *et al.* 1997). For this reason, it was used in the present work to characterise the general statolith elemental composition in *N. reticulatus* adults and by this way to perform a preliminary assessment regarding the possibility to: (i) detect annual growth rings that could be used to estimate the age of the animals; (ii) search for trace metal contamination that could be subsequently applied in environmental monitoring.

### 3.3 Material and methods

One statolith from each of three adult specimens of *Nassarius reticulatus* were used to determine statolith elemental composition in this species by EPMA. Two animals, sampled at Aveiro seacoast (40°38'50"N 8°47'08"W), provided statoliths S.1 and S.2. One more specimen, collected inside Ria de Aveiro estuarine system (40°30'39.26"N 8°44'55.64"W), provided statolith S.3. After sampling, animals were frozen and kept at -20°C until further processing. Statoliths were extracted from thawed specimens, as described in chapter 2. In order to digest any remaining flesh tissue from the statocyst, each statolith was placed on a single concave glass slide and immersed in a drop of saturated sodium hydroxide (NaOH) during three hours. Then, NaOH was completely removed and substituted by distilled water. This washing step was repeated twice and followed by two similar steps for dehydration: at first by immersion in 70% ethanol and then in 100% ethanol. Afterwards, glass slides containing statoliths were placed inside an oven at 60°C to dry for about 5 minutes.

Dried statoliths were embedded in resin (EpoFix kit from Struers) and mounted in plain glass slides whose surface was previously sanded, washed with detergent, rinsed abundantly with water and cleaned with absolute ethanol, in order to increase adhesion of resin to glass. The resin was prepared by mixing the 2 constituents of the EpoFix kit in the proportion 8 EpoFix resin : 1 EpoFix hardener. To get rid of air bubbles formed while mixing, the resin was kept for 2 minutes inside an oven at 60°C and then left standing at room temperature for 15 minutes. After that, a drop of resin was gently deposited on each glass slide and each statolith was positioned inside the resin and left at room temperature to polymerize for at least 24 hours. Subsequently, all statoliths were photographed under a light optical microscope (Zeiss) equipped with a camera (Moticam2300) and their maximum diameter measured.

EPMA requires the exposure of the statolith center to the surface. So, the resin was sanded with Silicon carbide powder p1000 in water, always controlling the statolith maximum diameter under the microscope so it does not pass its center. Once achieved the center, the statolith surface was washed with distilled water and dried with 100% ethanol. Then, the surface was polished on a Planopol grinder polisher (Struers), holding

the glass slide with the hand and pressuring the surface being polished to the rotating cloth on the equipment at 75 rpm. Different diamond polishing pastes (DP-Pastes from Struers) were used, decreasing in grain ( $6\mu\text{m}$ ,  $1\mu\text{m}$  and  $\frac{1}{4}\mu\text{m}$ ) in order to obtain a completely plain, light and bright surface for the EPMA. Each polishing paste was added to the respective Planapol cloth (one for each paste) and each statolith was polished during 3 to 4 minutes. A lubricant solution was also added to each cloth to avoid statoliths cracking and breaking. To remove pastes residues between different grains, glass slides were cleaned with 96% ethanol. At the end of the polishing process, glass slides were not only cleaned with 96% ethanol but also degreased by sonication in analytical grade ethanol for 15 minutes and then placed inside an oven at  $40^{\circ}\text{C}$  to dry for 5 minutes.

Perfectly polished, cleaned and bright statoliths were then metalized with carbon atoms (by vaporization) to guarantee the material electrical conductivity, and afterwards analysed by EMPA. In summary, this technique consists in projecting a finely focused electron beam (electron probe), of a diameter less than  $1\mu\text{m}$ , onto the point of the solid surface whose chemical composition is to be examined. Subsequently, the very small volume of material irradiated ( $<1\mu\text{m}^3$ ) emits a complex X-ray spectrum which includes the characteristic radiations of the various elements present at that point. Spectrographic analysis of this X-ray spectrum allows the respective concentrations of these elements to be determined (Castaing 1960). EMPA analysis was performed in a JEOL 8500-F electron probe microanalyser. This equipment is outfitted with 5 Wavelength Dispersive Spectrometers and has installed 12 analyzing crystals (PET, TAP, LIF and LDEs) that cover the whole spectrum from Beryllium ( $Z=4$ ) to Uranium ( $Z=92$ ). For rapid qualitative analysis it has also installed a high sensitivity SDD type Energy Dispersive Spectrometer. Chemical composition is determined by comparing the intensity of X-rays (number and energy/wavelength) from standards of known composition with those from unknown materials, correcting for the effects of atomic number, absorption and fluorescence in the sample using CITZAF correction program (Armstrong Program). The protocol for analysis was as follows.

Initially, the general composition of the sample was assessed by the Energy Dispersive X-ray Spectrum (EDS) acquired at 15kV, of a significant area of the statolith

exposed surface. This energy was chosen in order to have excited  $K\alpha$  lines of heavier elements. To improve resolution, a Wavelength Dispersive X-ray Spectra (WDS) were also obtained under the same conditions. The spectra revealed the presence of major and minor elements that were then included in the analysis program. Before analysis, a backscattered electron image (COMP image) was acquired at 10kV and 10nA with the same conditions as the quantitative analysis. Whenever possible, 3 analyses (3 points) by increment were performed, including the statolith nucleus. The analytical conditions for the quantitative analysis involved an acceleration voltage of 10kV, a beam current of 10nA and a beam diameter of 1 $\mu$ m. Line profiles for those elements along the statolith radius were also performed, searching for the occurrence of periodical cycles. These line profiles were carried out at an acceleration voltage of 15kV and a beam current of 20nA.

As Ba has been described as a trace element in statoliths of some gastropods larvae (Zacherl *et al.* 2003a; Zacherl *et al.* 2003b; Zacherl 2005; Lloyd *et al.* 2008), useful as a natural tag to track larval dispersal, its occurrence was also sought in one of the *Nassarius reticulatus* (L.) statoliths (S.3). In addition, some metallic elements – aluminium (Al), copper (Cu), mercury (Hg) and tin (Sn) – known to be environmental pollutants and so potentially capable of being deposited in statoliths, were also assessed in S.3. In these cases, longer measurement times (100s), an acceleration voltage of 10Kv and a higher beam current of 30nA were applied.

The standards used for quantitative analyses were: orthoclase ( $KAlSi_3O_8$ ) for Al, barite ( $BaSO_4$ ) for Ba, calcite ( $CaCO_3$ ) for Ca, cuprite ( $Cu_2O$ ) for Cu, cinnabar (HgS) for Hg, periclase (MgO) for Mg, albite ( $NaAlSi_3O_8$ ) for Na, pyrite ( $FeS_2$ ) for S, cassiterite ( $SnO_2$ ) for Sn and tausonite ( $SrTiO_3$ ) for Sr. As elements were determined as oxides, O concentrations were calculated by subtraction.

### **3.4 Results and discussion**

As mentioned in chapter 2, statoliths are typically spherical and exhibit a set of concentric layers deposited around a nucleus. In *N. reticulatus* this nucleus is produced during embryonic life and its formation is completed by the appearance of the

metamorphic ring at larval settlement (Barroso *et al.* 2005b; Chatzinikolaou and Richardson 2007). Thus, the term 'ring' refers to the dark segment of a bipartite structure called increment (Chatzinikolaou and Richardson 2007), which in fact corresponds to a light band together with the adjacent dark ring. These increments are repeatedly deposited around the nucleus, generating the statolith typical pattern, as can be observed in COMP images of Figures 36A to 36C for S.1 to S.3, respectively.

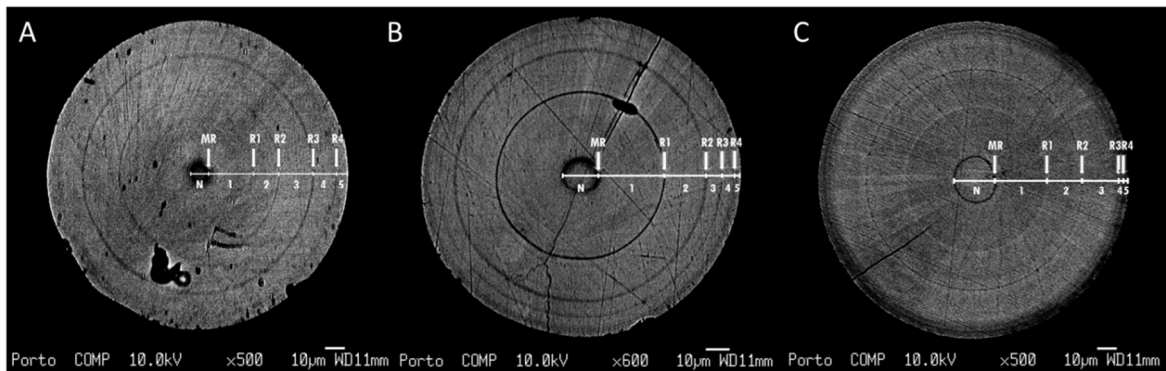


**Figure 36.** *Nassarius reticulatus*. COMP image showing general aspect of S.1 (A), S.2 (B), S.3 (C), indicating visible rings (MR, R1, R2, R3 and R4) and increments (1, 2, 3, 4 and 5), from the nucleus (N) to the statolith edge. MR: Metamorphic ring; R1: First ring; R2: Second ring; R3: Third ring; R4: Fourth ring; N: Nucleus; 1: First increment; 2: Second increment; 3: Third increment; 4: Fourth increment; 5: Fifth increment.

All statoliths analysed show the same structural pattern: there is a nucleus delimited by a metamorphic ring (MR) and, in addition to this core, four other rings are observed (R1, R2, R3 and R4). Thus, the nucleus (N) is surrounded by 5 increments: increment "1" from the MR to R1; increment "2" from R1 to R2; increment "3" from R2 to R3; increment "4" from R3 to R4; increment "5" from R4 to the statolith edge (see Figure 36).

Energy and wavelength dispersive X-ray spectra (EDS in Figure 37 and WDS in Figure 38) confirmed C, Ca and O as major elements in *Nassarius reticulatus* statoliths, corroborating the reported by other authors (Barroso *et al.* 2005b). Furthermore, the spectra also revealed the presence of some minor elements, namely: Mg, Na, S and Sr.

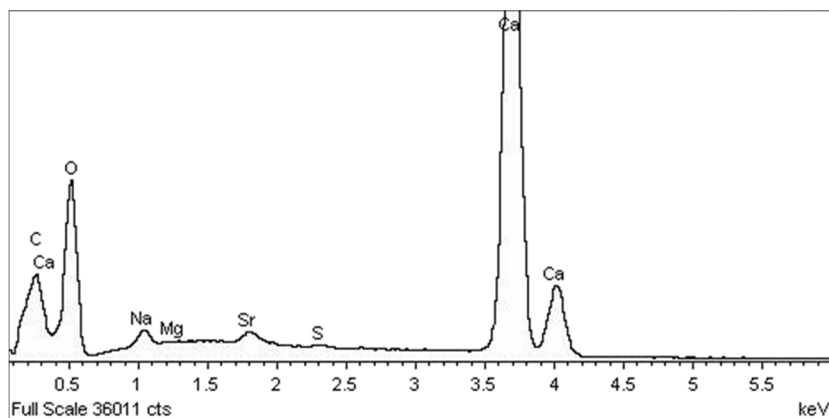


Figure 37 EDS Spectrum indicating the most representative elements in *Nassarius reticulatus* statoliths. C: Carbon; Ca: Calcium; Mg: Magnesium; Na: Sodium; O: Oxygen; S: Sulfur; and Sr: Strontium.

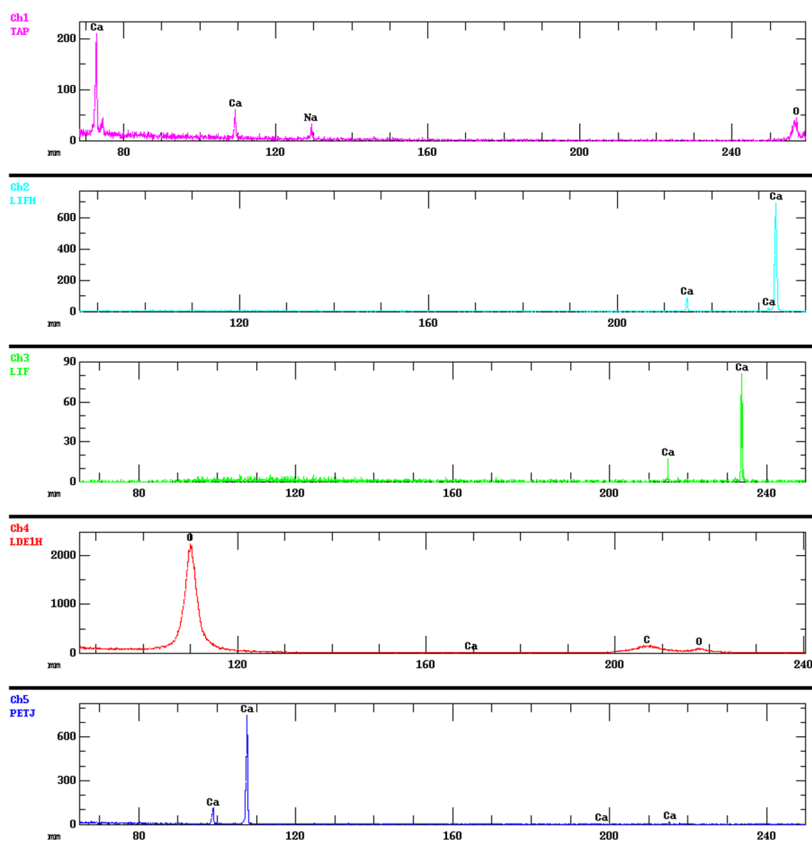


Figure 38 WDS Spectra indicating the most representative elements present in *Nassarius reticulatus* statoliths. C: Carbon; Ca: Calcium; Na: Sodium; O: Oxygen

Worth mentioning that spectra did not indicate the presence of Cl, as mentioned for *Aplysia californica* statoconia (Wiederhold *et al.* 1989) and *Helix lucorum* statoconia

(Gorgiladze 2002); nor of K and Si as for *H. lucorum* statoconia (Gorgiladze 2002); neither P as it was described for statoliths of *Strombus gigas* larva (Salley 1986).

Maximum and minimum concentrations for Ca, Mg, Na, O, S and Sr by statolith are presented in Table 4. We were unable to quantify C under this protocol since our surfaces were metalized with atoms of this element to guarantee the material electrical conductivity. Generally, concentrations of Ca and O are of the same order of magnitude ( $1 \times 10^5$  ppm), as well as of the pair Na and Sr ( $1 \times 10^3$  ppm) and Mg and S ( $1 \times 10^2$  ppm).

**Table 4 Elemental analysis of *Nassarius reticulatus* adult statoliths (S.1, S.2 and S.3) by EPMA. Maximum (Max) and minimum (min) concentrations detected for each element (ppm) within the set of analyses performed**

		Element (ppm)					
		Ca	Mg	Na	O	S	Sr
<b>S.1</b>	<b>Max</b>	419800	863	6063	171600	1079	8873
	<b>Min</b>	385800	202	4019	158400	469	5948
<b>S.2</b>	<b>Max</b>	414400	757	5858	169300	1309	2325
	<b>Min</b>	371500	346	3743	152700	576	1307
<b>S.3</b>	<b>Max</b>	422300	211	3799	171800	907	6777
	<b>Min</b>	403000	198	2541	163800	484	3896

Data on the chemical composition of *Helix lucorum* statoconia are of the same order of magnitude as our results for Ca, O, Na and S (Gorgiladze 2002). However, we cannot compare absolute values since different analytical methods were applied and results are on different biogenic structures (statoconia and statolith) and in different species. In *Nassarius reticulatus* statoliths, Ca and O are effectively the most representative elements: Ca was found at higher concentrations, varying from 371500 to 422300 ppm, while O ranged between 152700 and 171800 ppm (Table 3). Sodium concentrations varied from 2541 and 6063; Sr from 1307 and 8873 ppm; S from 469 and 1309 ppm; and Mg, which was not always detected, ranged from 198 to 863 ppm.

Mean concentrations of these elements by increment (N, 1, 2, 3, 4 and 5) are shown in Tables 5, 6 and 7 for S.1, S.2 and S.3, respectively. It should be noted that the

narrowness of N in S.1 (Figure 36a and Table 5), of increment 5 in S.2 (Figure 36b and Table 6) and of increments 4 and 5 in S.3 (Figure 36c and Table 7) did not allow quantitative analyses at these areas. In EPMA, analyses are performed in points of  $\approx 1\mu\text{m}$  (the electron beam diameter) although an interaction volume of  $\approx 3\mu\text{m}$  must be considered. Hence, the interaction volume in the aforementioned cases would certainly imply the quantification of elements contained not only in the light band of the increment (as in all other cases) but also in the adjacent dark ring, thus misleading the results.

**Table 5 Elemental analysis of statolith S.1 by EPMA. Mean concentrations of each element (ppm) by increment (see Figure 1) and respective coefficient of variation (CV). The value shaded in grey (Mg concentration in increment 4) was only detected at one of the three points analysed.**

Increment	Element (ppm)											
	Ca		Mg		Na		O		S		Sr	
	Mean	CV	Mean	CV	Mean	CV	Mean	CV	Mean	CV	Mean	CV
1	400000.0	0.03	442.5	0.42	4262.8	0.06	164000.0	0.02	790.0	0.27	7211.2	0.14
2	394466.7	0.04	523.0	0.61	4535.3	0.07	161566.7	0.03	644.0	0.25	6563.3	0.08
3	398233.3	0.03	443.3	0.30	4722.3	0.07	163733.3	0.02	716.7	0.20	8575.0	0.02
4	398500.0	0.03	607.0		4971.7	0.11	163566.7	0.02	790.7	0.15	7514.7	0.07
5	398733.3	0.04	451.0	0.49	5308.7	0.13	164366.7	0.04	1014.7	0.06	7710.7	0.05

**Table 6 Elemental analysis of statolith S.2 by EPMA. Mean concentrations of each element (ppm) by increment (see Figure 2) and respective coefficient of variation (CV).**

Increment	Element (ppm)											
	Ca		Mg		Na		O		S		Sr	
	Mean	CV	Mean	CV	Mean	CV	Mean	CV	Mean	CV	Mean	CV
N	388800.0	0.01	629.0	0.00	3753.5	0.00	158200.0	0.01	616.0	0.09	2048.5	0.17
1	395100.0	0.04	617.0	0.14	4698.7	0.06	161533.3	0.04	922.3	0.14	1720.3	0.10
2	389700.0	0.06	450.0	0.37	5471.3	0.06	159366.7	0.05	849.7	0.16	1496.3	0.13
3	378600.0	0.00	446.5	0.25	5560.5	0.02	155450.0	0.00	1063.5	0.24	1722.5	0.05
4	376100.0	0.02	697.0	0.12	5238.0	0.04	154500.0	0.02	1164.0	0.18	1864.5	0.35

**Table 7 Elemental analysis of statolith S.3 by EPMA. Mean concentrations of each element (ppm) by increment (see Figure 3) and respective coefficient of variation (CV). The value shaded in grey (Mg concentration in increment 3) was only detected at one of the three points analysed. -: not detected.**

Increment	Element (ppm)											
	Ca		Mg		Na		O		S		Sr	
	Mean	CV	Mean	CV	Mean	CV	Mean	CV	Mean	CV	Mean	CV
N	416333.3	0.01	-	-	3121.7	0.17	169266.7	0.01	540.3	0.10	6203.0	0.08
1	409466.7	0.01	-	-	3402.3	0.08	166600.0	0.01	751.3	0.01	4338.7	0.12
2	411866.7	0.02	202.0	0.03	3176.7	0.01	167700.0	0.02	771.7	0.15	4960.3	0.15
3	410966.7	0.01	211.0	-	3340.3	0.19	167466.7	0.01	699.0	0.17	5784.0	0.13

Statistical comparisons on elemental composition of different increments were performed using software SigmaStat v3.5. Kolmogorov-Smirnov test for normality and Levene's test for homoscedasticity were significant in some cases and thus, a non-parametric Kruskal-Wallis one way ANOVA on Ranks and the Dunn's Post-Hoc test were used to compare concentrations of each element in different increments by statolith. Results are presented in table 8.

**Table 8 Statistical comparisons of each element concentration between different increments of statoliths S.1, S.2 and S.3. - : not performed.**

Element	S.1		S.2			S.3			
	Kruskal-Wallis		Dunn's test			Kruskal-Wallis		Kruskal-Wallis	
	H	p	Comp	Q	p	H	p	H	P
Ca	1.842	0.765	-	-	-	5.679	0.224	2.077	0.557
Mg	1.088	0.896	-	-	-	5.244	0.263	-	-
Na	10.193	0.037*	1 vs. 5	2.914	<0.05*	9.346	0.053	1.513	0.679
O	2.004	0.735	-	-	-	5.159	0.271	2.179	0.536
S	7.544	0.110	-	-	-	6.987	0.137	6.897	0.075
Sr	8.275	0.082	-	-	-	4.436	0.350	7.308	0.063

In general, no significant differences in these elements concentrations were detected between increments. The only exception was Na concentration in statolith S.1, which presents a significant difference between increments 1 and 5, being higher in the last increment (compare Table 4 and Table 8).

Regarding the occurrence of periodical cycles, no particular pattern was evident. Figure 39 shows the line profiles for C, Ca, O and Sr in S.3 (the most representative elements in S.3), with the indication of the dark rings along the statolith radius, as an example of what was done to understand if any elemental pattern could be described. Likewise, Mg and S profiles (not shown in Figure 39 but also analysed) did not reveal any specific pattern along the statolith radius.

These are intriguing results since the annual periodicity of growth rings in the statoliths of *Nassarius reticulatus* was already proved (Chatzinikolaou and Richardson 2007) and so it was expected that at least some of the major elements would show a periodical pattern along the statolith radius. However, there are no well marked peaks and instead several peaks are spread along the profiles: not even at rings, regions claimed to be produced annually when animals stop growing at the cold season (Barroso *et al.* 2005a; Barroso *et al.* 2005b; Chatzinikolaou and Richardson 2007), any consistent decrease is observed. In the example of S.3 (Figure 39), Ca decreases slightly at the MR and increases at R1, having any particular variation in R2 and R3 and decreasing in R4. Oxygen decreases in R1 which coincides with the increase of Ca. Yet several other peaks are observed along the Ca profile, for example around 18 and 38 $\mu$ m from the profile start, where no ring is observed in the COMP image (within increments 1 and 2, see Figure 36).

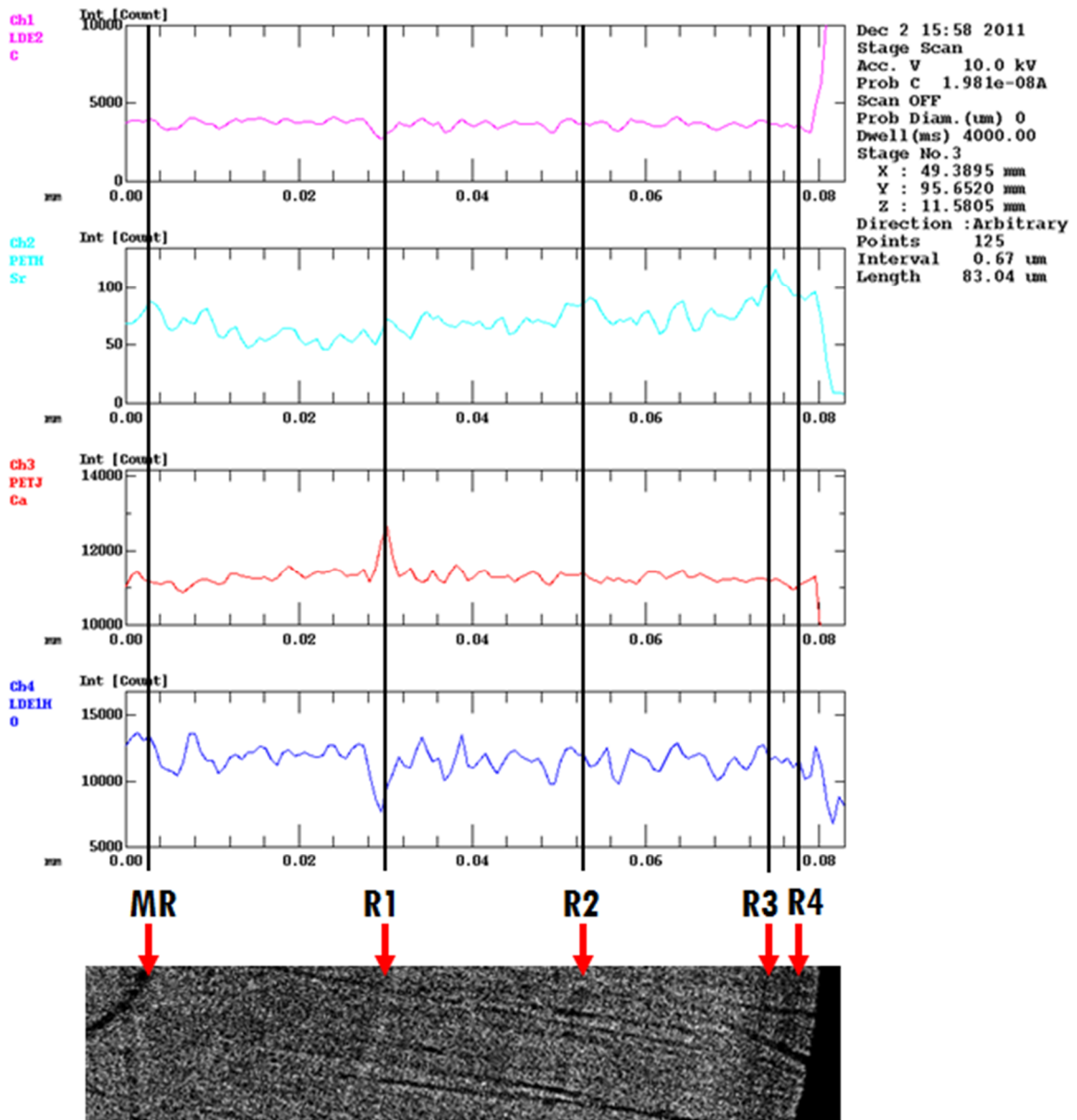


Figure 39 Line profiles of C, Sr, Ca and O along S.3 radius. Overlapping profiles (black vertical lines) are indicated the S.3 dark rings position. On the bottom of the figure there is also part of Figure 35 (S.3 COMP image) indicating the exact position of S.3 dark rings (MR, R1, R2, R3 and R4).

The presence of other minor / trace elements – Al, Ba, Cu, Hg and Sn – was also sought in increments 1, 2 and 3 of statolith S.3. Tin was not detected in any of the nine punctual analyses conducted (three per increment). Aluminium and Hg were only detected at 22.2% of the points analysed (2 out of 9) while Cu was at 66.7% (6 out of 9)

and Ba at 88.9% (8 out of 9). Concentrations of Al, Ba, Cu and Hg by increment are presented in Table 9.

**Table 9 Minor and trace elements in statolith S.3 detected by EPMA. Mean concentrations of each element (ppm) by increment (see Figure 3) and respective coefficient of variation (CV). (\* the values are not means since the element was only detected at one of the three analyses carried out at each increment. -: not detected).**

Increment	Element (ppm)							
	Al		Ba		Cu		Hg	
	Mean	CV	Mean	CV	Mean	CV	Mean	CV
1	55.0*		664.5	0.21	301.5	0.50	-	
2	71.0*		969.3	1.17	274.3	0.40	180.0*	
3	-		647.3	0.11	183.0		176.0*	

We should have a critical view on these results since it seems that more appropriate techniques have been suggested for the accurate quantification of trace elements in this kind of biogenic structures. Campana (1997; 1999) showed that there are significant differences in determining otoliths elemental composition by using different analytical procedures. The author suggested that the major elements (C, Ca and O) can be truthfully determined by several methods but minor elements such as Na can only be accurately measured with an electron microprobe, while trace elements quantification require proton-induced X-ray emission (PIXE) or inductively coupled plasma mass spectrometry (ICP-MS). The author also pointed the reduced sensitivity of most beam-based assays compared to their solution-based counterparts, in part due to the much lower sample weights being analysed. Not only did the sensitivity of the solution-based techniques extend over a broader range of elements, but the precision of those assays was significantly better than those of the beam-based methods (Campana 1997; Campana 1999). In fact, looking at our results, Mg was detected in the EDS spectrum as a minor element and we were not able to quantify it in some analyses (see Table 5 and 7)

whereas increasing measurement times and beam current allowed the detection and quantification of Ba and Cu in concentrations higher than those obtained for Mg in S.3 (Table 7 and 9).

Of course that such a comparison of precision is not strictly valid, since the probed procedures incorporate the biogenic material heterogeneity which is not present in the solution-based methods. Actually, EPMA allows punctual analysis, without material loss and in specific areas, but what is an advantage in some cases can be of no value in others. EPMA allowed us to determine concentrations by increment, from the nucleus to the statolith edge, what is impossible by other analytical methods such as ICP-MS since the entire sample is consumed during analysis. Nonetheless, we cannot assume neither that the elements we quantified are the only ones present within our samples nor conclude that, because we could not detect for example Sn, this element is not present in statoliths.

Even so, these technique allow the characterization of *Nassarius reticulatus* adult statoliths and accurately measured the most representative elements – Ca, O, Sr, Na and S – along the structure all radius.

### **3.5. The gastropod statolith organic matrix**

There are also references for the presence of an organic matrix in gastropods statoliths, although it was not possible to find a definite work on such issue as there is for cephalopods statoliths (Radtke 1983) and fish otoliths (see review by Campana 1999).

D'Asaro (1965) noted that, after *S. gigas* veligers fixation in Bouin's acidic solution, all that was left of the statolith was a 'layered organic matrix'. Some years later, Salley (1986) referred that the use of acetic acid have dissolved the mineral component of statoliths leaving behind a shrivelled organic (outer) matrix, but just in some of the *S. gigas* larvae analysed. The author has then pointed, as a possible explanation for inconsistency, that the organic matrix sheathing the statolith might form an impermeable coat, while in some statoliths a deformation of this outer layer could render their

permeability to the acid (Salley 1986). Apart from these records, though without checking chemical nor organic composition, Gorgiladze *et al.* (2010) stated that statoconia are microscopic biomineral structures formed by growth layers of mineral and organic origin. Nevertheless, these authors referred a previous work showing, by phase contrast microscopy, that statoconia consisted of alternating dark and light concentric layers around an optically dense oval core (or nucleus), often with radial streaks seen more or less clearly (Gorgiladze 2002). Actually, this internal microstructure of prominent and clearly defined concentric growth rings have been demonstrated in suitably prepared gastropod statoliths of *Concholepas concholepas* (Zacherl *et al.* 2003a), *Littorina scabra* (Bell 1984), *Nassarius reticulatus* (Barroso *et al.* 2005b; Chatzinikolaou and Richardson 2007), *Neptunea antiqua* (Richardson *et al.* 2005a), *Polinices pulchellus* (Richardson *et al.* 2005b), *Strombus costatus* (Grana-Raffucci and Appeldoorn 1997) and *Strombus gigas* (Salley 1986; Grana-Raffucci and Appeldoorn 1997). Hence, the gastropod statolith have been proposed for age and growth studies (Bell 1984; Grana-Raffucci and Appeldoorn 1997; Barroso *et al.* 2005b; Richardson *et al.* 2005a; Richardson *et al.* 2005b; Chatzinikolaou and Richardson 2007), being also pointed as having particular potential for many others applications, namely understanding aspects of the life history and ecology of gastropods, issues previously provided only by fish and cephalopods.

### 3.6 References

- Barroso, C. M., Moreira, M. H., Richardson, C. A. (2005a) Age and growth of *Nassarius reticulatus* in the Ria de Aveiro, north-west Portugal. *Journal of the Marine Biological Association of the United Kingdom* 85: 151-156.
- Barroso, C. M., Nunes, M., Richardson, C. A., Moreira, M. H. (2005b) The gastropod statolith: a tool for determining the age of *Nassarius reticulatus*. *Marine Biology* 146: 1139-1144.
- Bell, J. L. (1984) Statoliths as age indicators in gastropod larvae - Application to measurement of field growth-rates. *Pacific Science* 38: 357-357.
- Campana, S. E. (1997) Use of radiocarbon from nuclear fallout as a dated marker in the otoliths of haddock *Melanogrammus aeglefinus*. *Marine Ecology-Progress Series* 150: 49-56.
- Campana, S. E. (1999) Chemistry and composition of fish otoliths: pathways, mechanisms and applications. *Marine Ecology-Progress Series* 188: 263-297.
- Campana, S. E., Thorrold, S. R., Jones, C. M., Gunther, D., Tubrett, M., Longerich, H., Jackson, S., Halden, N. M., Kalish, J. M., Piccoli, P., dePontual, H., Troadec, H., Panfili, J., Secor, D. H., Severin, K. P., Sie, S. H., Thresher, R., Teesdale, W. J., Campbell, J. L. (1997) Comparison of accuracy, precision, and sensitivity in elemental assays of fish otoliths using the electron microprobe, proton-induced X-ray emission, and laser ablation inductively coupled plasma mass spectrometry. *Canadian Journal of Fisheries and Aquatic Sciences* 54: 2068-2079.
- Castaing, R. (1960) Electron Probe Microanalysis. In: Marton L, Claire M (eds) *Advances in Electronics and Electron Physics*. Academic Press, pp 317-386.
- Chatzinikolaou, E., Richardson, C. A. (2007) Evaluating growth and age of netted whelk *Nassarius reticulatus* (Gastropoda: Nassariidae) using statolith growth rings. *Marine Ecology-Progress Series* 342: 163-176.
- Chia, F. S., Koss, R., Bickell, L. R. (1981) Fine structural study of the statocysts in the veliger larva of the nudibranch, *Rostanga pulchra*. *Cell and Tissue Research* 214: 67-80.
- D'Asaro, C. N. (1965) Organogenesis, development, and metamorphosis in the queen conch, *Strombus gigas*, with notes on breeding habits. *Bulletin of Marine Science* 15: 359-416.
- Gallin, E. K., Wiederhold, M. L. (1977) Response of *Aplysia* statocyst receptor cells to physiologic stimulation. *The Journal of Physiology* 266: 123-137.
- Gao, W., Wiederhold, M., Hejl, R. (1997) Development of the statocyst in the freshwater snail *Biomphalaria glabrata* (Pulmonata, Basommatophora). *Hearing Research* 109: 125-134.
- Gao, W., Wiederhold, M. L. (1997) The structure of the statocyst of the freshwater snail *Biomphalaria glabrata* (Pulmonata, Basommatophora). *Hearing Research* 109: 109-124.
- Gorgiladze, G. I., Bukia, R., Davitashvili, M., Taktakishvili, A., Gelashvili, N., Kalandarishvili, E., Satdykova, G. (2010) Morphological Peculiarities Statoconia in Statocysts of Terrestrial Pulmonary Snail *Helix Lucorum*. *Bulletin of Experimental Biology and Medicine* 149: 269-272.

- Gorgiladze, G. I. (2002) Weightlessness Stimulates Growth of Statoconia. *Doklady Biological Sciences* 384: 216-220.
- Grana-Raffucci, F. A., Appeldoorn, R. S. (1997) Age determination of larval strombid gastropods by means of growth increment counts in statoliths. *Fishery Bulletin* 95: 857-862.
- Lloyd, D. C., Zacherl, D. C., Walker, S., Paradis, G., Sheehy, M., Warner, R. R. (2008) Egg source, temperature and culture seawater affect elemental signatures in *Kelletia kelletii* larval statoliths. *Marine Ecology-Progress Series* 353: 115-130.
- McKee, A. E., Wiederhold, M. L. (1974) *Aplysia* statocyst receptor cells: fine structure. *Brain Research* 81: 310-313.
- Pedrozo, H. A., Schwartz, Z., Dean, D. D., Harrison, J. L., Campbell, J. W., Wiederhold, M. L., Boyan, B. D. (1997) Evidence for the Involvement of Carbonic Anhydrase and Urease in Calcium Carbonate Formation in the Gravity-Sensing Organ of *Aplysia californica*. *Calcified Tissue International* 61: 247-255.
- Radtke, R. L. (1983) Chemical and structural characteristics of statoliths from the short-finned squid *Illex illecebrosus*. *Marine Biology* 76: 47-54.
- Richardson, C. A., Saurel, C., Barroso, C.M., Thain J (2005a) Evaluation of the age of the red whelk *Neptunea antiqua* using statoliths, opercula and element ratios in the shell. *Journal of Experimental Marine Biology and Ecology* 325: 55-64.
- Richardson, C. A., Saurel, C., Kingsley-Smith, P. R., Seed, R., Chatzinikolaou, E. (2005b) Age and growth of the naticid gastropod *Polinices pulchellus* (Gastropoda: Naticidae) based on length frequency analysis and statolith growth rings. *Marine Biology* 148: 319-326.
- Salley, S. (1986) Development of the Statocyst of the Queen Conch larva, *Strombus gigas* L. (Gastropoda: Prosobranchia). Institute of Oceanography, Faculty of Graduate Studies and Research, Montreal, Canada.
- Wiederhold, M. L., Sharma, J. S., Driscoll, B. P., Harrison, J. L. (1990) Development of the statocyst in *Aplysia californica* I. Observations on statoconial development. *Hearing Research* 49: 63-78.
- Wiederhold, M. L., Sheridan, C. E., Smith, N. K. R. (1989) Function of molluscan statocysts. In: Crick R (ed) *Fifth International Symposium on Biomineralization*. Plenum Press, New York, pp 393-408.
- Zacherl, D. C. (2005) Spatial and temporal variation in statolith and protoconch trace elements as natural tags to track larval dispersal. *Marine Ecology-Progress Series* 290: 145-163.
- Zacherl, D. C., Manriquez, P. H., Paradis, G., Day, R. W., Castilla, J. C., Warner, R. R., Lea, D. W., Gaines, S. D. (2003a) Trace elemental fingerprinting of gastropod statoliths to study larval dispersal trajectories. *Marine Ecology-Progress Series* 248: 297-303.
- Zacherl, D. C., Paradis, G., Lea, D. W. (2003b) Barium and strontium uptake into larval protoconchs and statoliths of the marine neogastropod *Kelletia kelletii*. *Geochim Cosmochim Acta* 67: 4091-4099.

## Chapter 4 – Conclusion

The statolith, on gastropods, in the four subclasses studied on the present work (chapter 2), is only present on subclass Caenogastropoda. The fact that species of subclass Caenogastropoda have one statolith instead of statoconia makes them more interesting for the study of sclerochronology. In all caenogastropods species the statolith can be characterized as round, translucent, with concentric rings.

The statocyst are close to pedal ganglia, in caenogastropods are dorsal to pedal ganglia and in the others subclasses, Patellogastropoda, Vetigastropoda and Heterobranchia, are between pleural and pedal ganglia. The statocyst structure, of *N. reticulatus* (Caenogastropoda), is a transparent vesicle with a round shape like the found on heterobranchs. The main difference between the statocyst that have statoliths and the statocyst that have statoconia is the number and size of the receptor cells (Stahlschmidt and Wolff 1972; Mckee and Wiederhold 1974; Pedrozo *et al.* 1996; Gao and Wiederhold 1997).

It was verified that, in the specie *Nucella lapillus*, the statolith follows the growth of the animal from the embryo to adulthood. A statolith with 3 rings was observed in an embryo with 24<sup>th</sup> days. It was concluded that the statolith, in this specie, is formed before the 3<sup>rd</sup> week, probably in the beginning of the second week, as reported on Lloyd *et al.* (2008) for the specie *Kelletia kelletii*. The statolith growth is parallels to the species growth. This was already reported for *N. reticulatus* collected from Aveiro by Barroso *et al.* (2005b).

The particularity, of the statolith increment follows the growth of the animal throughout life, lead us to want to know the statolith composition, because the statolith may probably provide an important register of physical and chemical characteristics of the marine environment.

The general composition of statoliths radius from adults *N. reticulatus* was characterized: Ca, O, Sr, Na and S. No significant differences in the different elements concentration between the increments were found. About the occurrence of periodical cycles in the statolith rings, there were no evidences of a particular pattern.

The rings in the statolith are related with the age of the species. In spite of the results with the electron microprobe do not demonstrate the presence of seasonality in the rings, Barroso *et al.* (2005b) has proven that the statoliths rings are annual rings. In fact, Barroso *et al.* (2005b) was the first work that demonstrated that adult gastropods statoliths of *N. reticulatus* had potential for sclerochronology.

The study of adult gastropod statoliths is just beginning and there are many hypothesis to be tested, namely if statoliths can be accurately used as pluriannual chronometers; if they are good indicators of environmental pollution; and if, for example, these two properties can be combined to use gastropods statoliths as archives to reconstruct marine pollution histories. Some of these hypotheses have been successfully tested in analogous structures such as fish otoliths (Campana 1999) and cephalopods statoliths (Zumholz 2005) and also in some gastropods through monitoring annual rings production monthly in wild animals (Barroso *et al.* 2005a).

The hypothesis of using gastropods statoliths as biomarkers of marine pollution has huge interest for environmental pollution monitoring namely in coastal waters. In comparison with the open coast, near shore waters along coastal margins and estuaries are often rich in pollutants of anthropogenic origin (Bruland 1983) resulting in elevated concentrations of many elements in hard parts (as it has been shown for otoliths, considered as metabolically inert timekeepers and environmental recorders; Campana 1999). Otoliths annular structure examination offers the possibility of evaluate contaminants incorporation over time, providing a historic record of past and recent exposure of fish to contaminants (Campana 1999). However, fishes are highly mobile and this approach has been applied mainly to track migratory and dispersion routes (Milton and Chenery 2001; Swearer *et al.* 2003). Contrariwise, as referred above, gastropods are sedentary or poorly mobile organisms, a pre-requisite for selecting them as good pollution indicators. Furthermore, the gastropod statolith is less complex than the cephalopods counterpart and their microstructure is already proved to allow age determination and to evaluate growth (Bell 1984; Grana-Raffucci and Appeldoorn 1997; Barroso *et al.* 2005b; Richardson *et al.* 2005a; Richardson *et al.* 2005b; Chatzinikolaou and Richardson 2007). Nevertheless, and despite the recognition of their great potential to

reconstruct marine pollution histories, there is still a long way to go until their validation as true *biorecorders* of environmental changes.

## 4.1 References

- Barroso, C. M., Moreira, M. H., Richardson, C. A. (2005a). Age and growth of *Nassarius reticulatus* in the Ria de Aveiro, north-west Portugal. *Journal of the Marine Biological Association of the United Kingdom* 85: 151-156.
- Barroso, C. M., Nunes, M., Richardson, C. A., Moreira, M. H. (2005b) The gastropod statolith: a tool for determining the age of *Nassarius reticulatus*. *Marine Biology* 146: 1139-1144.
- Bell, J. L. (1984) Statoliths as age indicators in gastropod larvae - Application to measurement of field growth-rates. *Pacific Science* 38: 357-357.
- Bruland, K. W. (1983) Trace elements in seawater. In: Riley JP, Chester R (eds) *Chemical oceanography*. Academic Press, London, pp 157-220.
- Campana, S. E. (1999) Chemistry and composition of fish otoliths: pathways, mechanisms and applications. *Marine Ecology-Progress Series* 188: 263-297.
- Chatzinikolaou, E., Richardson, C. A. (2007) Evaluating growth and age of netted whelk *Nassarius reticulatus* (Gastropoda: Nassariidae) using statolith growth rings. *Marine Ecology-Progress Series* 342: 163-176.
- Grana-Raffucci, F. A., Appeldoorn, R. S. (1997) Age determination of larval strombid gastropods by means of growth increment counts in statoliths. *Fishery Bulletin* 95: 857-862.
- Lloyd, D. C., Zacherl, D. C., Walker, S., Paradis, G., Sheehy, M., Warner, R. R. (2008) Egg source, temperature and culture seawater affect elemental signatures in *Kelletia kelletii* larval statoliths. *Marine Ecology-Progress Series* 353: 115-130.
- Milton, D. A., Cheney SR (2001) Sources and uptake of trace metals in otoliths of juvenile barramundi (*Lates calcarifer*). *Journal of Experimental Marine Biology and Ecology* 264: 47-65.
- Richardson, C. A., Saurel, C., Barroso, C.M., Thain J (2005a) Evaluation of the age of the red whelk *Neptunea antiqua* using statoliths, opercula and element ratios in the shell. *Journal of Experimental Marine Biology and Ecology* 325: 55-64.
- Richardson, C. A., Saurel, C., Kingsley-Smith, P. R., Seed, R., Chatzinikolaou, E. (2005b) Age and growth of the naticid gastropod *Polinices pulchellus* (Gastropoda: Naticidae) based on length frequency analysis and statolith growth rings. *Marine Biology* 148: 319-326.
- Swearer, S. E., Forrester, G. E., Steele, M. A., Brooks, A. J., Lea, D. W. (2003) Spatio-temporal and interspecific variation in otolith trace-elemental fingerprints in a temperate estuarine fish assemblage. *Estuarine, Coastal and Shelf Science* 56: 1111-1123.
- Zumholz, K. (2005) The influence of environmental factors on the micro-chemical composition of cephalopod statoliths. Leibniz Institute of Marine Sciences IFM-GEOMAR, Kiel.